THESIS FOR THE DEGREE OF LICENTIATE OF ENGINEERING

Antibacterial elastomeric materials for biomedical applications

ANNIJA STEPULANE

Department of Chemistry and Chemical Engineering

CHALMERS UNIVERSITY OF TECHNOLOGY

Gothenburg, Sweden 2022

Antibacterial elastomeric materials for biomedical applications

ANNIJA STEPULANE

Technical report Nr 2022:14
Department of Chemistry and Chemical Engineering
Division of Applied Chemistry
Chalmers University of Technology
SE-412 96 Gothenburg
Sweden
Telephone + 46 (0)31-772 1000

Cover: An illustration of the material modification strategies developed in this thesis. From left: PDMS surface modification with hydrogel microparticle coating with contact killing and drug-eluting properties, followed by PDMS-hydrogel blend with drug-eluting properties.

Printed by Chalmers Reproservice
Gothenburg, Sweden, December 2022

Antibacterial elastomeric materials for biomedical applications

ANNIJA STEPULANE

Department of Chemistry and Chemical Engineering

Division of Applied Chemistry

Chalmers University of Technology

Abstract

An ageing population in combination with scientific and clinical advancements have led to a steady increase in the use of medical devices. Elastomeric biomaterials – materials displaying rubber-like mechanics – have found widespread applicability in the production of both short- and long-term medical devices. Despite the prevalence of such devices, issues with medical device-associated infections remain. By surface colonization of bacteria, systemic infection can arise resulting in patient suffering and increased burden on the healthcare system. Consequentially, development of antibacterial elastomers capable of withstanding bacterial surface colonization has been proposed as an effective strategy for prevention and mitigation of medical device-associated infections.

In this thesis, two alternative strategies to develop antibacterial polydimethylsiloxane (PDMS) elastomers have been proposed and evaluated. In the first strategy, PDMS surface modification with multifunctional hydrogel microparticle coating has been developed. Using a coating of antimicrobial peptide (AMP) RRPRPRPRPWWWW-NH_2 functionalized hydrogel particles, high antibacterial activity was reported against *Staphylococcus epidermidis* and *Staphylococcus aureus*. As an additional functionality, the ability of the coating to encapsulate and release therapeutic substances was investigated, resulting in a sustained delivery of polar, amphiphilic, and nonpolar drugs.

In the second strategy, modification of bulk PDMS by synthesis of drug-eluting PDMS-hydrogel blends was proposed. PDMS and triblock copolymer (diacrylated Pluronic F127, DA-F127) hydrogel blends were prepared with varying ternary PDMS–DA-F127–H_2O compositions. The test compositions chosen resulted in stable elastomers with tailorable mechanics and ordered self-assembled nanostructure. The variation in composition offered potential for sustained delivery of polar and nonpolar drugs, demonstrating potential for production of drug-eluting and antibacterial elastomeric devices with tailorable mechanics.

Keywords: polydimethylsiloxane, hydrogels, antibacterial coating, elastomer blends, antimicrobial peptides, drug-delivery

List of publications

This thesis contains the following publications appended to the thesis:

Paper I

Multifunctional Surface Modification of PDMS for Antibacterial Contact Killing and Drug-Delivery of Polar, Nonpolar and Amphiphilic Drugs

Annija Stepulane, Anand Kumar Rajasekharan, Martin Andersson

ACS Applied Bio Materials, 2022, accepted and available online

https://doi.org/10.1021/acsabm.2c00705

Paper II

Elastomeric Liquid Crystals

Annija Stepulane, Kajsa Ahlgren, Adrian Rodriguez Palomo, Anand Kumar Rajasekharan, Martin Andersson

Submitted

Contribution report

Paper I: Main author. Performed all experiments and analysis except for Raman and X-ray photoelectron spectroscopy measurements. Wrote the first draft of the manuscript.

Paper II: Main author. Supervised all the experimental work except for synchrotron small-angle X-ray scattering measurements. Wrote the first draft of the manuscript.

Acknowledgments

I would like to thank Knut and Alice Wallenberg foundation through their Wallenberg Academy Fellow program and the Area of Advance for Materials Science at Chalmers University of Technology for funding this project.
I would like to say the biggest thank you to every person involved in the work (both directly and indirectly) that has gone into this thesis.
To my supervisor Martin Andersson for all the support and encouragement during these, sometimes challenging, years. Thank you for believing me, especially when I struggled to do so myself. Your motivation and uplifting attitude have taught me to see great value in the work we have done together.
To my co-supervisor Anand Kumar Rajasekharan for your patient and methodical approach, fruitful scientific discussions, and mental support during these past years.
To my examiner Hanna Härelind, thank you for all the time invested during my PhD education and the positive and encouraging attitude.
To my co-authors Kajsa Ahlgren and Adrian Rodriguez Palomo for the fun and productive work done together on Paper 2.
To Katarina Logg from Chalmers Materials Analysis Laboratory (CMAL) for help with Raman spectroscopy and Andreas Schaefer at Applied Chemistry for assistance with XPS measurements.
To all MA research group members, both current and previous (Edvin, Mats, Gustav, Maja, Jenny, Florian as well as current and previous master students) for fostering a fun, friendly, comfortable, and mentally stimulating environment.
To Amferia AB team (Saba, Rojan and Daniel) for everyday support, as well as scientific advice in all-things microbiology. Thank you for your interest and support in my PhD, even though my presence might have seemed random at times. I am doing my PhD, I promise.
To my boyfriend Paul. For all the love, happiness and support that have fuelled me throughout this work. I could not have done this without you.

Gothenburg, December 2022
Annija Stepulāne

Abbreviations

AMP	Antimicrobial peptide
CFU	Colony forming unit
DA-F127	Diacrylated Pluronic F-127
EDC	1-Ethyl-3-(3-dimethylaminopropyl) carbodiimide
IBP	Ibuprofen
IPN	Interpenetrating polymer network
LLC	Lyotropic liquid crystal
MQ	Milli-Q water
NHS	N-hydroxysuccinimide
PBS	Phosphate buffered saline
PDMS	Polydimethylsiloxane
RMSE	Root mean square error
SAXS	Small angle X-ray scattering
SEM	Scanning electron microscopy
TSB	Tryptic soy broth
UV-Vis	Ultraviolet-visible
VCM	Vancomycin
WCA	Water contact angle
XPS	X-ray photoelectron spectroscopy

Table of contents

1. Introduction

The advent of medicine has provided humankind with treatment strategies for many diseases that 100 years ago would have resulted in permanent deficiencies or even death. We as humans live longer and healthier compared to our predecessors. A combination of prevention, early diagnosis, and better treatment strategies have significantly improved the recovery from even the most life-threatening conditions like infections, cancer and trauma. The discovery of new drugs, with antibiotics as the most consequential example, is an obvious component of modern medicine. However, the significance of medical devices cannot be overstated. A medical device can be defined as any article that is not a drug, capable of aiding in diagnosis, treatment, mitigation or prevention of a disease, as well as restoration and support of a bodily function. Ranging from short-term assisting devices like needles, surgical tools, and band aids, to intermittent function-supporting devices like urinary catheters and pulmonary ventilators, to life-supporting devices like orthopaedic implants and cardiac pacemakers, medical devices are ubiquitous in modern-day medical care.

From a material science point of view, medical devices have integrated all biomaterial classes – polymers, metals, and ceramics – with great success. However, major challenges associated with practical applications remain, the most common being medical device associated infections. When a medical device comes in contact with human body, more often than not, it will be recognized as foreign, initiating a cascade of immune system responses. With the material surface being the direct contact point with the tissue and physiological fluids, a conditioning film of proteins and other organic molecules will deposit from blood, urine, saliva etc. Although aiding the body in the recognition of the material, and determining the further immune response to the device, the material surface is also being rendered favourable for attachment of bacteria. With bacterial colonization being the most common cause of medical device associated infections, bacterial attachment and proliferation onto the material surface remains a challenge to address.

Depending on the invasiveness and contact duration of a device, formation of bacterial biofilms can occur resulting in systemic infection (*e.g.* 1% in hip and knee prosthesis, 70% – 80% in urinary catheters) [1, 2]. The current approach for prevention and treatment of device-associated bacterial infections utilizes antibiotic therapy; however, once formed, biofilms are difficult to eradicate, resulting in limited efficiency of the drug [3]. Moreover, the global burden of antimicrobial resistance exacerbates antibiotic-resistant infections associated with the use of medical devices [4, 5]. In consequence, the need for new and improved strategies for device-associated infection prevention are highly relevant.

A potential alternative for managing these infections is the development of antibacterial biomaterials capable of withstanding bacterial colonization. Fundamentally antibacterial material properties can be achieved via multiple material-modification routes (*e.g.* bacteria-repelling, contact-killing, bactericide releasing) [6]. The two modification strategies utilized in this thesis deal with: 1) delivery of antibacterial agents from the material structure, and 2) immobilization of antibacterial agents as surface coatings.

1.1. Aim and objectives

This thesis addresses the development of antibacterial elastomeric biomaterials; rubber like materials found in a variety of biomedical applications. Polydimethylsiloxane (PDMS) is a commonly utilized elastomer for production of urinary catheters, medical tubing, soft tissue implants and contact lenses, however, is inherently prone to bacterial attachment, facilitating the need for development of antibacterial modification strategies.

The aim of this thesis was to develop modification strategies to PDMS to impart antibacterial properties for use in medical device production. Here, two alternative strategies have been investigated:

1. Modification of pristine PDMS surface with contact killing hydrogel microparticle coating with capacity for localized drug delivery.
2. Synthesis of new PDMS-hydrogel blends with local drug delivery capacity.

The proposed modification strategies are illustrated in **Figure 1**.

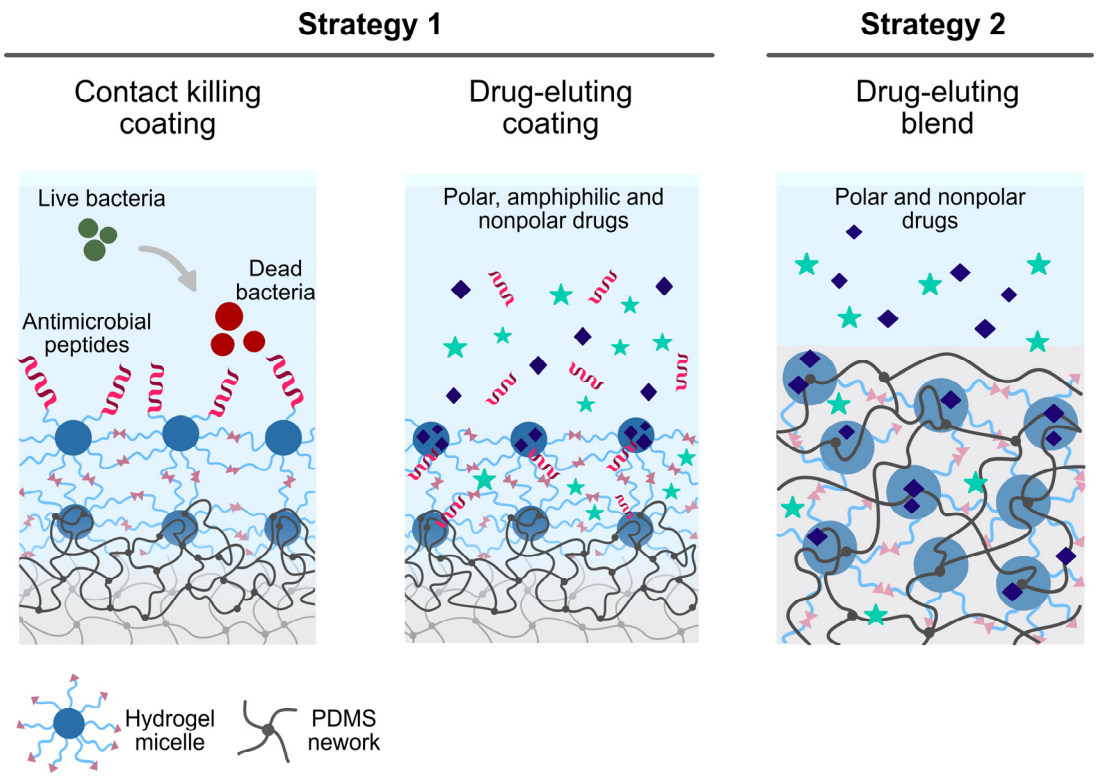

Figure 1. Proposed PDMS modification strategies. In strategy 1, PDMS surface has been functionalized with amphiphilic hydrogel microparticle coating for contact killing and drug-eluting properties. In strategy 2, drug-eluting PDMS-hydrogel blends have been synthesized.

2. Theoretical background

The following sections address the relevant scientific background on the two antibacterial PDMS modification strategies investigated in this thesis – contact killing hydrogel microparticle coating development and synthesis of drug-eluting PDMS blends. First, a brief overview of PDMS elastomers, their relevant properties and the practical implications of the said properties will be summarized. Secondly, the existing antibacterial PDMS modification strategies will be reviewed. Next, the development of contact killing PDMS modification with the help of antimicrobial peptides (AMP) and amphiphilic hydrogel coatings will be presented as the first strategy. Finally, the development of drug-eluting PDMS blends as the second strategy will be introduced.

2.1. PDMS materials for biomedical applications

Polydimethylsiloxane is a silicone-based elastomer commonly used for a variety of biomedical applications. Due to its bio-inert properties, crosslinked PDMS elastomers have been utilized for production of contact lenses, shunts, prosthesis, urinary catheters, burn dressings, heart valve structures, aesthetic and orthopaedic implants etc. [7-9]. This variety of applications stems from PDMS material properties, where high flexibility, elasticity, thermal and chemical resistance is combined with UV resistance, high gas permeability and optical transparency. Also, PDMS is relatively easy to fabricate and can be sterilized using autoclave, steam or gamma radiation, making it an attractive candidate for medical device manufacturing [7].

From a biocompatibility point of view, medical grade PDMS elastomers are nontoxic, non-irritating and considered as biocompatible with soft and hard tissues, as well as being hemocompatible [10]. A key PDMS property is the high surface hydrophobicity (water contact angle ~ 101° – 109°) that is believed to contribute to blood compatibility and resistance to encrustation [7].

Despite this, PDMS materials pose complications in use of biological systems due to the low surface energy and intrinsic hydrophobicity, resulting in nonspecific adsorption of proteins and other biomolecules. Originating in the entropic gain from water molecule displacement adjacent to the surface, protein adsorption leads to protein conditioning film formation *in vivo,* harbouring a favourable environment for bacterial attachment [11].

Upon formation of the conditioning film, PDMS surface serves as a target for bacterial attachment and colonization. By secretion of extracellular matrix components, complex biofilm communities can form, encasing the bacteria in a protective matrix. Once formed, biofilms are very difficult to eradicate due to the significantly increased

bacterial tolerance to antibiotics, resulting in systemic infection [12]. Consequently, novel antibacterial PDMS modification strategies are of great interest to address the infection formation at its onset.

2.2. Antibacterial PDMS modification strategies

Considerable research efforts have been invested in development of biomaterials capable of preventing infections. To date, a large variety of PDMS modification strategies have been reported that utilizes a surface or bulk material modification to either prevent initial bacterial attachment or eradicate established colonization.

To hinder bacterial attachment, antifouling PDMS surface have been produced by grafting of zwitterionic polymer brushes or polyzwitterionic coatings. Through formation of a stable water hydration layer that hinders protein conditioning, bacterial adhesion to PDMS surface can be minimized [13-15].

Alternatively, antifouling properties can be achieved via surface topography modifications where micro- or nanoscale surface features can be utilized to interfere with the ability of bacteria to attach and form biofilms. Multiple studies have successfully utilized soft lithography techniques to produce patterned PDMS surfaces capable of inhibiting the growth of gram-negative *Escherichia coli* [16, 17].

Another approach for infection prevention entails the use of antibacterial agent integrated with the material. By impregnation into the material structure or immobilization onto the surface, local antibacterial effect can be achieved. A large variety of antibacterial compounds have been applied in combination with silicone elastomers by either adsorption, absorption, or covalent immobilization. Conventional antibiotic eluting silicone catheters have shown to prevent colonization of both gram-positive and gram-negative bacteria species up to 12 weeks [18, 19]. Although promising, challenges with sustained delivery of effective concentration remains an issue to address in drug-eluting materials. Historically, silver coated silicone catheters have been developed due to silver's bactericidal properties with multiple commercial products available [20, 21]. However, their clinical efficacy and safety remains controversial, motivating the need for new alternatives [22, 23].

2.3. Contact killing PDMS coatings

Lately, a group of contact killing antibacterial agents have gained attention for the development of antibacterial PDMS materials. Contact killing antibacterial agents can generally be characterized as a class of molecules capable of bacterial membrane disruption through charged and/or hydrophobic interactions upon close contact. Consequently, surface immobilization of contact killing surface coatings has been

suggested as an effective strategy, since they do not release any active substances, limiting the concerns related to toxicity and resistance [24].

For example, PDMS surfaces modified with contact killing chitosan derivatives have been reported, capable of supressing biofilm formation via combination of increased surface hydrophilicity and positive charge [25, 26]. Alternatively, PDMS modification with quaternary ammonium compounds have been demonstrated, where contact killing effect is achieved by a combination of high cationic charge density and hydrophobicity [27]. Antimicrobial peptides, a class of molecules known for their rapid, broad spectrum, highly specific antibacterial activity, have been applied in the development of contact killing PDMS surfaces. Multiple studies have utilized a variety of covalent immobilization techniques of AMPs onto PDMS, resulting in retained antibacterial activity against both gram-positive and gram-negative bacteria species [28-30]. Covalent AMP immobilization is of specific importance in the modification of PDMS surface with contact killing hydrogel microparticle coating investigated in this thesis, therefore AMPs, their properties and motivation for covalent immobilization will be addressed in the following section.

2.3.1. Antimicrobial peptides

AMPs, also known as host-defence peptides, are a class of small organic molecules, that are naturally abundant in animal and plant kingdom. In mammalian organisms, AMPs are a part of nonspecific immune response towards bacteria, fungi, viruses, and protozoa. Having evolved in cohabitation with microorganisms, AMPs have retained their high antimicrobial activity without emergence of resistance due to their unique mode of action, where AMPs target the fundamental differences distinguishing microbial cellular membranes from multicellular plants and animals [31].

Although AMPs possess a large variety in molecular structures, certain motifs are universal that enable their antibacterial properties. In general, AMP molecules have an amphiphilic character through spatial organization of non-polar amino acids and cationic polar amino acids. The charge and amphiphilicity contributes to peptide activity, where it is believed that electrostatic attraction between the negatively charged bacterial membrane and positively charged AMP molecules is vital. Both gram-positive and gram-negative bacterial cell membranes contain anionic phospholipid moieties, that are absent in mammalian cells, granting AMPs with selectivity [32]. Upon electrostatic attraction, the hydrophobic peptide domains penetrate the phospholipid bilayer of the bacterial membrane, facilitating membrane disruption. Subsequentially, membrane integrity is impaired, leading to the cytoplasmic contents to spill out and cells to lyse. Although this model of AMP membrane activity is universally accepted, it is worth

noting that more detailed membrane disruption theories are available, depending on the specific AMP structure [31-33].

Additionally, there exist AMPs that, much like antibiotics, affect specific molecular targets in the bacterial cell for exertion of antibacterial effect *e.g.*, DNA/RNA synthesis, protein synthesis, cell wall synthesis, cell division, and protein folding [34]. However, it is still believed that membrane activity plays a key role in their functionality.

In this thesis, a synthetically derived AMP has been utilized belonging to the proline/arginine-rich end leucine-rich repeat protein (PRELP) family with the following amino acid sequence – RRPRPRPRPWWWW-NH_2 (RRP9W4N) as seen in **Figure 2**. In a previous study performed by Malmsten *et al.* arginine (R) and proline (P) rich RRPRPRPRP sequence was end-tagged with hydrophobic amino acid tryptophan (W) residues, concluding that 4 tryptophan residues results in high antimicrobial activity in combination with low toxicity to mammalian cells [35]. With an overall net positive charge of +6 and a hydrophobic tryptophan end-tag, RRP9W4N is reported to retain high membrane activity with moderate haemolysis potential [36].

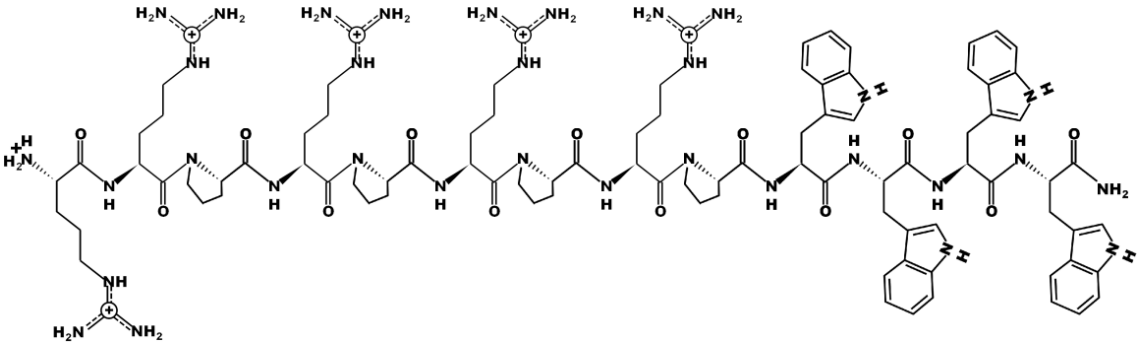

Figure 2. Antimicrobial peptide RRP9W4N structure utilized in this thesis.

2.3.2. Covalent immobilization of antimicrobial peptides

Despite the potential of antimicrobial peptides as discussed above, clinical applications of AMPs pose certain challenges associated with peptide stability, *i.e.* susceptibility to high salt concentration and proteolytic degradation, as well as high production costs [32]. These factors have facilitated the need for engineering new materials that help AMPs to improve their functionality in clinically relevant applications. Covalent immobilization of AMPs onto biomaterials has been deemed as a suitable alternative for enhancing their stability *in vitro* and *in vivo*. By covalent attachment of AMPs, increased stability towards proteolytic degradation can be achieved, resulting in non-leaching surfaces capable of circumventing the challenges associated with antibiotic eluting materials [37].

Depending on the chemical structure of the peptide and the chosen material platform, a variety of chemical conjugation techniques have been applied for covalent AMP immobilization [37, 38]. The immobilization strategy utilized in this thesis relies on peptide bond formation between AMP and the hydrogel microparticle coating. Through reaction between primary amines found in AMP structure and surface bound free carboxyl groups, stable AMP coating can be achieved. For this reason, carbodiimide conjugation chemistry has been utilized by reaction with 1-ethyl-3-[3-dimethylaminopropyl] carbodiimide hydrochloride (EDC) and *N*-hydroxysuccinimide (NHS) resulting in direct AMP to substrate peptide bond formations (see **Figure 3**).

It is worth noting that multiple factors have been identified to affect the efficacy of covalently immobilized AMPs, e.g. coupling chemistry, material properties of substrate, use of spacer molecules as well as density of AMP grafting and corresponding orientation [32]. Although interesting, closer analysis of these factors is outside the scope of this thesis.

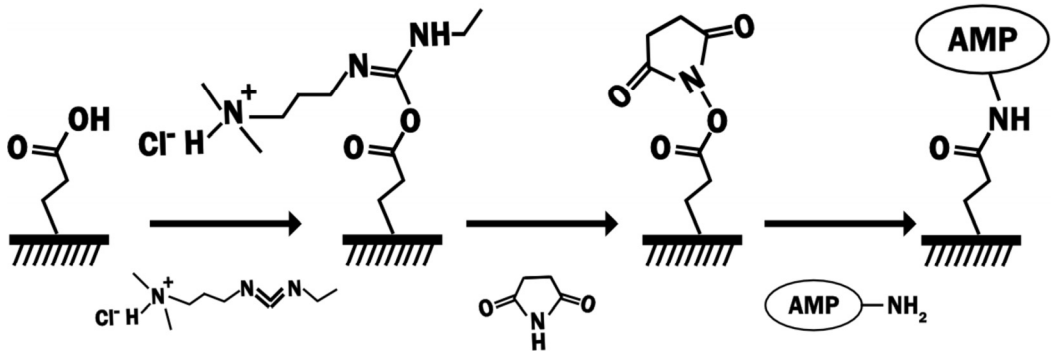

Figure 3. AMP covalent immobilization strategy via peptide bond formation to surface free carboxyl groups using EDC/NHS activation chemistry; here, the hydrogel microparticle coating onto PDMS functions as the AMP immobilization platform.

2.3.3. Hydrogel microparticle coating on PDMS

Previous studies have identified RRP9W4N potential for covalent immobilization onto amphiphilic hydrogels in wound-care applications, with high antibacterial potential reported against *Staphylococcus epidermidis*, *Staphylococcus aureus*, *Pseudomonas aeruginosa*, methicillin-resistant *Staphylococcus aureus,* and multidrug-resistant *Escherichia coli* strains [39, 36]. Although hydrogel materials possess many beneficial properties relevant in biomedical applications, they lack the mechanical integrity characteristic of elastomeric biomaterials like PDMS. Additionally, direct AMP attachment onto pristine PDMS can be chemically complex due to the chemical inertness of PDMS surfaces. Therefore, in this thesis hydrogels have been utilized in

the form of surface coatings deposited onto PDMS to function as an immobilization platform for covalent RRP9W4N attachment.

For this reason, an amphiphilic Pluronic F127 based hydrogel has been utilized. Pluronic F127 is a triblock copolymer consisting of poly(ethylene oxide) (PEO) and poly(propylene oxide) (PPO) segments endowing it with amphiphilic, surfactant-like behaviour. Pluronics are well known for their ability to self-assemble in a variety of lyotropic liquid crystal (LLC) phases depending on concentration, temperature and presence of segment selective solvents [40]. Additionally, due to the large variety of LLC morphologies, Pluronic F127 has been used as a drug delivery vehicle for delivery of polar and nonpolar drugs [41, 42].

Here, previously reported, RRP9W4N modified hydrogel microparticles made out of diacrylated version of Pluronic F127 (DA-F127) were utilized for the production of the particle coating onto PDMS (see **Figure 4**) [36]. Use of microparticle coating could be motivated by increase in coating surface area, resulting in improved antibacterial effect, as well as circumventing the issues associated with thin uniform monolith hydrogel coating delamination.

2.3.4. Drug-eluting hydrogel microparticle coating on PDMS

To endow the hydrogel particle coating with additional functionality, DA-F127 microparticles were investigated for their ability to selectively entrap polar, amphiphilic, and nonpolar drugs in the hydrophobic and hydrophilic domains of the micellar cubic phase (**Figure 4**). As previously mentioned, Pluronic F127 hydrogels have been widely explored for their ability to deliver active substances of different chemical polarity due to the amphiphilic structure of the material [41-43].

In general, development of drug delivery systems and drug-eluting biomaterials has become of particular interest due to therapeutic advantages like sustained therapeutic effect and reduced frequency of dosing. Contrary to the systemic administration, localized drug delivery circumvents the toxic side effects with additional specificity to the target tissue [44]. Localized delivery of antibacterial agents from biomaterials is of particular interest in addressing medical device associated infections [45]. By tailoring of material properties and the resulting drug delivery characteristics, existing infections could be treated by delivery of antibacterial agent to the infection site [20].

In this thesis, three model drugs have been utilized to investigate the hydrogel particle coating capacity for drug delivery. Here the antibiotic vancomycin, antimicrobial peptide RRP9W4N and anti-inflammatory drug ibuprofen were utilized as polar, amphiphilic, and nonpolar model drugs, respectively. By releasing the drugs from the

particle coating, a potential strategy for antibacterial PDMS modification could be achieved.

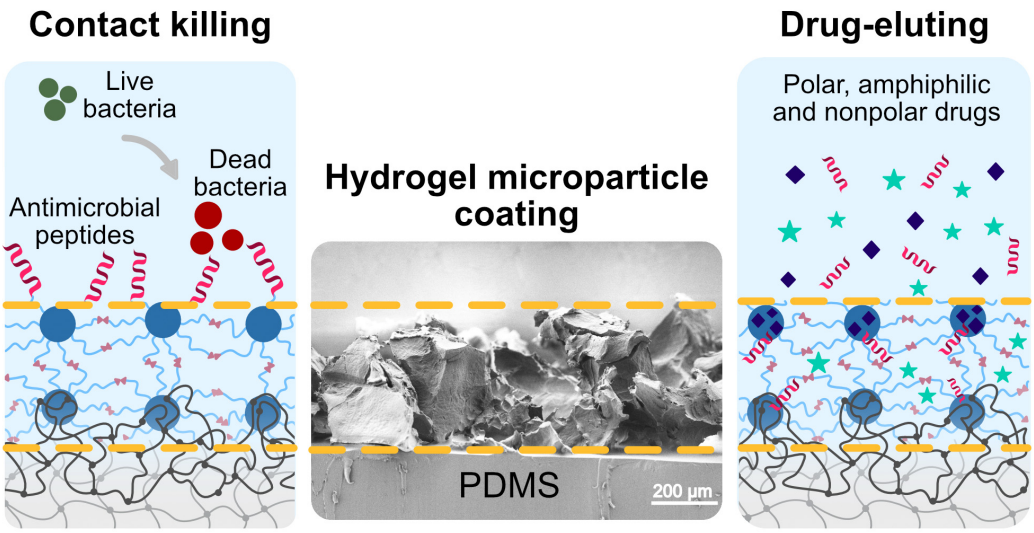

Figure 4. Proposed modification strategy of PDMS surface with contact killing hydrogel microparticle coating, with localized drug delivery capacity of polar, amphiphilic and nonpolar drugs.

2.4. Drug-eluting PDMS blends

Although the development of antibacterial surface coatings can be perceived as an attractive strategy for production of antibacterial elastomers, challenges associated with the chemical stability of coatings and the longevity of the antibacterial effect *in vivo* must be considered. In an ideal scenario, an elastomer could be able to deliver antibacterial properties without the need of surface modification, motivating the need for new antibacterial elastomeric biomaterial synthesis. This thesis attempts to address this need by synthesizing PDMS elastomer blends with local drug delivery capacity as the second alternative for development of antibacterial elastomers.

Polymer blending can be considered one of the oldest and most cost-effective strategy for the synthesis of new polymeric materials with different physical properties. By blending of two or more, often antagonistic polymers, blends of different characteristics can be achieved depending on the miscibility between the separate components. Fundamentally, blends can be classified as: 1) immiscible or heterogenous, where two or more distinct phases exist, 2) compatible, where an immiscible blend exhibits macroscopically uniform properties, and 3) miscible or homogenous, with single-phase structure [46]. Depending on these interactions' as well as the component concentration, different macro, micro or nanodomain polymer morphologies can be achieved [47].

Most often, due to the low interfacial adhesion between the blend phases, mechanically weak materials are formed, motivating the need for compatibilization strategies.

Silicone elastomers, like PDMS, are highly immiscible with most other organic polymers, making production of thermodynamically stable, homogenous silicone blends complex. A potential alternative for silicone blends with increased stability is the use of AB diblock or ABA triblock block copolymer compatibilization agents, where interfacial tension is reduced by selective miscibility between the polymer phases [48-50].

As mentioned previously, PDMS materials are highly hydrophobic with low surface energy making any surface or bulk modification challenging. Therefore, multiple studies have attempted to use silicone blending with hydrophilic polymers like polyethylene glycol (PEG) or amphiphilic block copolymers like Pluronics to improve PDMS functionality by *e.g.,* increasing surface wettability, water retention and permeability to active substances [51-53]. By inducing phase separation upon addition of hydrophilic entities, PDMS blends for use in controlled drug release systems and wound dressings have been developed.

To further investigate the PDMS blending, this thesis studies PDMS blends with Pluronic F127 and water, to produce elastomeric materials with drug delivery functionality. As referred to earlier, Pluronic F127 possesses a wide lyotropic liquid crystalline behaviour when mixed with block-selective solvents, resulting in molecular segregation [40]. Solvent and concentration variation gives rise to a realm of LLC morphologies *e.g.,* micellar cubic, reverse micellar cubic, normal hexagonal, reverse hexagonal and lamellar phases. Here, Pluronic F127 self-assembly was utilized with the intention for synthesis of LLC based elastomeric blends, with PDMS intended to function as the nonpolar, and water as the polar “solvents”. It was hypothesized that, upon introduction of amphiphilic copolymers, distinct polar and nonpolar domain formation could be induced, creating depots for encapsulation of polar and nonpolar drugs, resulting in a sustained release character compared to the hydrogel particle coating.

3. Materials and methods

The following section introduces the material synthesis and characterization methods covered in this thesis with respect to the preparation of 1) PDMS surfaces with contact killing hydrogel microparticle coating, and 2) PDMS elastomer blends. Furthermore, the methodology for *in vitro* drug release experiments is described for both the PDMS hydrogel microparticle coating and the PDMS blends. Finally, evaluation of antibacterial activity of the AMP modified PDMS coating will be summarized. A more detailed procedure description can be found in Paper 1 and Paper 2 appended to the thesis.

3.1. Material preparation

3.1.1. Coating preparation

For production of hydrogel microparticle coating onto PDMS developed in Paper 1, hydrogel particles were synthesized from DA-F127 hydrogel sheets using a detailed method stated elsewhere [36]. Briefly, 30% w/w DA-F127 in Milli-Q water (MQ) and 0.05% w/w photoinitiator Irgacure 2959 were mixed and crosslinked at $\lambda = 302$ nm using UV radiation forming solid hydrogels, which were then washed in excess water. The washed and hydrated hydrogel sheets were homogenized using a food processor and a homogenizer to produce microparticle suspension, followed by a washing step and suction filtration. The filter cake was collected, and the resulting particle paste divided into two parts: 1) control particles and 2) AMP functionalized particles. Control particles were frozen in liquid N_2, freeze-dried to remove excess water, and stored dry until further use.

The particles intended for AMP functionalization were treated with EDC and NHS for activation of free carboxyl groups, followed by covalent AMP attachment. For that 1 g of particles was dispersed in 5 ml of activation solution consisting of 2 mg/ml of 1-Ethyl-3-(3-dimethylaminopropyl) carbodiimide (EDC) and 2 mg/ml N-hydroxysuccinimide (NHS) solutions in 0.5 M 2-(N-morpholino) ethanesulfonic acid buffer (MES, pH 6) and stirred for 30 min, followed by suction filtration and washing with MQ water. The activated particles were dispersed in 5 ml 400 μM RRP9W4N AMP dissolved in phosphate buffered saline (PBS, pH 7.4) and stirred for 2 h for covalent AMP attachment, followed by excessive washing, filtration and freeze drying. To quantify the amount of AMP taken up by the particles, UV-Vis spectroscopy was utilized at $\lambda = 280$ nm to probe for tryptophan group using a previously constructed standard curve.

The freeze-dried control and AMP particles were further utilized for production of the particle coating onto PDMS substrates. For that, Sylgard 184 (Dow Corning) silicone elastomer kit was mixed in ratio ten parts base agent with one part curing agent to form a homogenous prepolymer gel. The gel was degassed to remove any trapped air bubbles, cast in a glass dish, and heat cured resulting in a solid elastomer. Next a new batch of PDMS prepolymer gel was mixed, degassed, and spun on top of the previously produced PDMS substrates using a spin coater (SPIN150-v3, SPS-Europe B.V.). Spinning procedure was carried out for 3 min with an acceleration rate of 500 rpm/s, whilst spin speed was varied between 1000 rpm to 6000 rpm in increments of 1000 rpm. Immediately afterwards, PDMS substrates were covered with the freeze-dried hydrogel particle powder and cured at 37 °C for 24 h. This procedure facilitated the absorption of the hydrophobic PDMS prepolymer into the hydrophobic domains of the DA-F127 hydrogel particle structure, forming interpenetrating polymer network upon curing, and stabilizing the particle coating onto PDMS.

3.1.2. PDMS blend synthesis

For production of drug-eluting PDMS blends further described in Paper 2, the PDMS prepolymer was directly mixed with DA-F127 gel and water, forming triphasic blend, followed by crosslinking into solid materials. A variety of PDMS–DA-F127–H_2O concentrations were mixed according to Pluronic F127-water-"oil" ternary systems reported previously, in order to investigate the concentration effect on the blend properties [40]. For that, different concentrations of DA-F127 gels were mixed as previously described by varying the water content. Afterwards, PDMS prepolymer was mixed as previously described and the two mixtures were combined by manual mixing according to the desired PDMS–DA-F127–H_2O concentration. The resulting unpolymerized gel mixtures were sandwiched between two glass slides followed by a two-step polymerization of (1) heat-curing at 37 °C for 24 hours and (2) UV curing at $\lambda = 365$ nm for 7 – 10 min. The heat- and photopolymerization were carried out to crosslink the PDMS and DA-F127 networks, respectively. The former is a platinum catalysed hydrosilylation reaction between the vinyl groups in the Sylgard 184 base agent and the silane groups in the curing agent forming PDMS, whilst the latter is a free-radical photopolymerization of the DA-F127 acrylate groups in the presence of photoinitiation.

3.2. Material characterization

3.2.1. Coating morphology and stability

The as-prepared and rehydrated particle coatings developed in Paper 1 were investigated to characterize the coating morphology and adhesion stability.

The as-prepared and rehydrated (in MQ water or safranin dye solution) particle coatings were imaged with a stereo microscope (Stemi 508, Carl Zeiss) to evaluate the particle coverage of the PDMS substrates. Contrary to regular microscopy, stereomicroscopy is able to visualize the test sample with increased depth of field aiding the investigation of three-dimensional objects like the particle coatings.

Particle size distribution of the as-prepared coating samples was measured from the generated stereo microscopy images to characterize the population of particles immobilized onto PDMS surface. Particle projection diameter was measured on three hundred randomly selected particles, and the corresponding number-based size distribution calculated.

To qualitatively evaluate the effect of spin speed, used for the particle coating, on the particle adhesion, Scotch™ tape (Magic™ Tape, 3M) peel-off test was performed. Four consecutive tape applications and removals were performed on the as prepared coatings and the coatings photographed for a side-by-side comparison. The peel-off test was utilized as a straight-forward method to characterize the adhesion strength of the particle coating to the PDMS substrate by providing repeatability and for qualifying the surfaces.

3.2.2. Scanning electron microscopy

Scanning electron microscopy (SEM) was utilized to image the morphology of the particle coating on PDMS as well as the PDMS blend microstructure. SEM is an imaging technique that uses focused electron beam to excite the electrons present in the analysed material structure, generating characteristic signals. In this work, secondary electron detection was utilized to produce surface topography images of the as-prepared particle coating from Paper 1 and to investigate the adhesion between the PDMS and hydrogel particles. Additionally, SEM was used to inspect the microstructure of the synthesized PDMS blends in Paper 2 by looking at sample cross-sections. Additionally, particle coating was incubated together with *Staphylococcus epidermidis* to qualitatively evaluate the AMP effect on the bacterial growth behaviour. Inoculated samples were fixed in formaldehyde, followed by dehydration steps in an ethanol and incubation in hexamethyldisilazane solution. All analysed samples were sputter coated with gold prior the SEM imaging.

3.2.3. Water contact angle analysis

Water contact angle (WCA) analysis was utilized to investigate the wetting properties of the particle coating on PDMS and the PDMS blends. For that optical tensiometer (Theta, Attention) was operated in static contact angle mode with MQ water. By monitoring the WCA changes over time with high resolution camera, surface

hydrophilicity/hydrophobicity and the underlying surface chemical properties can be investigated. In Paper 1 presence of AMP in particle coating was analysed by monitoring WCA changes over time on as-prepared coatings. In Paper 2, WCA was utilized to analyse the PDMS–DA-F127–H_2O concentration variation effect on the wetting properties of the PDMS blends, and the possible surface chemical characteristics.

3.2.4. Raman spectroscopy

Chemical characterization of the coating (Paper 1) was performed utilizing confocal Raman microscope (Alpha300 R, WITec). Raman in a light scattering analysis technique whereupon irradiating the test sample with a high intensity laser source, inelastic Raman scattering is produced. By measuring the generated signal, molecularly characteristic vibrational energy modes of different molecules present can be differentiated. By investigating the as-prepared control and AMP particle coatings, molecular bands characteristic to RRP9W4N could be detected, aiding in detection of AMP presence.

3.2.5. X-ray photoelectron spectroscopy

Surface chemistry of the coating, (Paper 1) was characterized using X-ray photoelectron spectroscopy (XPS) microprobe (PHI 5000 VersaProbe III, Ulvac-PHI Inc.). XPS is a surface-sensitive analysis technique for investigation of surface chemical composition. By exposing the sample to X-ray source, characteristic photoelectrons are emitted from the material surface yielding information on the electronic states of the atoms. In this study, XPS was used for elemental quantification of the control and AMP particle coating with particular interest in changes in nitrogen concentration, potentially indicating the presence of AMP in the material.

3.2.6. Tensile and compression testing

Tensile and compression testing was employed to characterize the PDMS blends developed in Paper 2. The purpose of mechanical testing was to evaluate how changes in PDMS–DA-F127–H_2O component concentration in the synthesized blends affect the mechanical properties of the materials. For that, Instron 5600 UTM universal testing machine was used with a 100 N and 5000 N load cell for tensile and compressive deformation, respectively. PDMS blend were synthesized as described in Section 3.1.2., with additional centrifugation step of the unpolymerized gel mixtures prior crosslinking, to remove any air bubbles. Pristine PDMS sheets and 30% w/w DA-F127 hydrogels were used as reference materials to account for their mechanical contribution.

To quantify the mechanical response, Young's and compressive moduli were calculated from the linear regions of the obtained stress-strain curves.

3.2.7. X-ray scattering

Small-angle X-ray scattering (SAXS) was used for structural characterization of the PDMS blends developed in Paper 2. In SAXS analysis sample is irradiated with a monochromatic X-ray source causing X-rays to be scattered based on the electron densities in the sample. By recording the scattered X-ray intensity, information on the nanostructure and ordering in the material can be obtained. In Paper 2, two types of SAXS instruments were used for analysis of unpolymerized gel mixtures and polymerized PDMS blends. A Mat:Nordic instrument (SAXSLAB, Chalmers Materials Analysis Laboratory, Sweden) was used for the unpolymerized gels, while synchrotron radiation SAXS was performed at the cSAXS beamline, Swiss Light Source (Paul Scherrer Institute, Switzerland) on the polymerized PDMS blends. The purpose of using SAXS was to study the possible short- and long-range nanostructure formations in the PDMS–DA-F127–H_2O systems, elucidating DA-F127 phase behaviour in the presence of PDMS and water as nonpolar and polar "solvents", respectively.

3.3. Antibacterial evaluation of the particle coating

AMP particle coating on PDMS developed in Paper 1 was investigated for its antibacterial activity against *Staphylococcus epidermidis* and *Staphylococcus aureus* – common pathogens involved in medical device associated infections. To compare the antibacterial activity, AMP-free control particle coating, as well as pristine PDMS substrates were included to serve as the negative controls.

Hydrated samples were incubated together with *S. epidermidis* or *S. aureus* cultures for 1h in 10% v/v tryptic soy broth (TSB) in PBS solution. Afterwards, the bacteria suspension was aspirated and replaced with pure 10% v/v TSB followed by an overnight incubation. This procedure granted early-stage biofilm formation onto the tested sample surfaces. The following day, samples were carefully washed to remove any planktonic bacteria and vortexed to remove the surface-adhered bacteria. The vortexed suspensions were serially diluted, and spot plated onto brain-heart infusion agar plates, followed by colony forming unit (CFU) counting the next day. By comparing the differences between the CFU counts obtained from AMP particle coating to control particle coating and pristine PDMS, AMP contact killing antibacterial effect could be evaluated.

3.4. *In vitro* drug delivery

The coating developed in Paper 1 and the PDMS blends developed in Paper 2 were investigated for their ability to encapsulate and release drugs of different chemical

polarity using vancomycin (VCM), RRP9W4N AMP and ibuprofen (IBP) as the polar, amphiphilic, and nonpolar mode drugs, respectively. The purpose of this was to assess how the addition of DA-F127 particle coating onto PDMS, and the DA-F127 addition in the PDMS blends would facilitate drug uptake into the materials' structure, granting PDMS with drug delivery capacity.

3.4.1. Drug delivery from the particle coating

Control particle coating on PDMS developed in Paper 1 was prepared as described in section 3.1.1. at a 1000 rpm spin speed, followed by a washing step and drying at 37 °C. The dried samples were loaded in 1% w/v AMP solution in MQ water, 1% w/v VCM solution in MQ water or 7% w/v IBP solution in acetone, alternatively, for 24 h to facilitate drug uptake int the particles via swelling. The drug-loaded samples were then rinsed in MQ water or acetone and dried at 37 °C for 24 h to remove any loosely bound drug.

For release studies MQ water was used as the elution media for VCM and AMP loaded coatings, while 1% w/v aqueous sodium dodecyl sulphate (SDS) solution was used for IBP loaded coating to facilitate IBP solubility. The elution volume was chosen accordingly, so the system would operate under the sink condition. The samples were continuously shaken, and the elution media sampled every 15 min for the first 4 h, then every 30 min for 8 h, following once daily until elution saturated. UV-Vis spectrophotometer (Multiskan™ GO, Thermo Fisher Scientific) was used to measure the sample absorption at $\lambda = 280$ nm, $\lambda = 280$ nm or $\lambda = 272$ nm for VCM, AMP or IBP, respectively, returning the sampled volume to the system after each measurement. To assess the PDMS substrate ability to encapsulate the different drugs, a control experiment was conducted using a pristine PDMS substrate.

3.4.1.1. Mathematical modelling

The drug release kinetics from the particle coating developed in Paper 1 was assess by mathematically fitting the release data to zero order, first order, Korsmeyer-Peppas and Higuchi drug delivery models. Non-linear least square regression was applied using DDSolver add-in program for modelling and comparison of drug dissolution profiles based on a built-in model library [54]. Model fit to the release data was expressed by using the correlation coefficient (R^2) and root mean square error (RMSE). To compare the release rate of different drugs, release rate constants were calculated. Ultimately, to characterize the release mechanism from the particle coatings, Korsmeyer-Peppas release exponent n was determined.

3.4.2. Swelling measurements of the PDMS blends

Swelling capacity of the PDMS blends developed in Paper 2 was investigated in aqueous media. As-prepared PDMS blend samples were swollen in MQ water with periodical weight checks, recording the swollen and dry sample weight, and the resulting mass swelling ratio $S_{w,t}$ was calculated. By monitoring the water swelling behaviour of the synthesized PDMS blends a better understanding of the material properties and the drug loading process could be obtained.

3.4.3. Drug delivery from the PDMS blends

PDMS blends synthesized in Paper 2 were prepared as described in section 3.1.2. with an additional chloroform wash and vacuum drying step. The dry samples were then loaded with 1% w/v VCM solution in MQ water or 10% w/v IBP solution in acetone, alternatively, for 72 h to facilitate drug uptake int the material structure, followed by an intermediate rinsing and drying step. MQ water and 1% w/v SDS solution was used as the elution media for VCM and IBP release, respectively. UV-Vis spectrophotometer at λ = 280 nm and λ = 272 nm was used to monitor the drug release for VCM and IBP, respectively, measuring every 15 min for the first 4 h, then twice a day for 3 days and once a day until no further elution could be recorded. The purpose of this was to investigate the PDMS blend composition effect on the drug delivery dose and retention time.

3.5. 3D printing of the PDMS blend

As a proof-of-concept experiment one PDMS blend developed in Paper 2 was chosen to demonstrate the material's processing capabilities via 3D printing. Unpolymerized gel was loaded into a syringe and centrifuged at 6000 rpm for 10 min to remove air bubbles. The syringe was placed in the printing cartridge and the unpolymerized gel printed using extrusion-based 3D bioprinter (INKREDIBLE™, Cellink). The printed constructs were polymerized following an inverse two-step polymerization procedure by photopolymerization with UV light (λ = 365 nm), followed by heat curing for 24 h at 37 °C.

4. Results and discussion

4.1. Material preparation

To produce hydrogel microparticle coating on PDMS described in Paper 1, the following production scheme was developed (**Figure 5**). The choice of DA-F127 hydrogel microparticles to produce the coating could be motivated by two reasons: (1) higher surface area for stronger surface adhesion, when compared to a coating based on a thin uniform monolith coating of DA-F127 hydrogel and (2) increase in the coating surface area for improved antibacterial effect.

PDMS prepolymer film was spin-coated onto pristine PDMS surface for immobilization of the freeze-dried hydrogel particle powder. The spin coated PDMS layer was intended to act as an immobilization matrix and adhesive entrapping the particles and forming a robust coating. The DA-F127 hydrogel particles utilized in this work had a micellar cubic phase granting the material with distinct hydrophilic and hydrophobic domains. Due to the amphiphilic nature of hydrogel particle, uptake of the hydrophobic PDMS prepolymer could occur via swelling, forming interpenetrating polymer network (IPN) structure between the particles and PDMS. This structure was further immobilized by heat curing of PDMS resulting in stable physical bond between hydrogel particles and PDMS network.

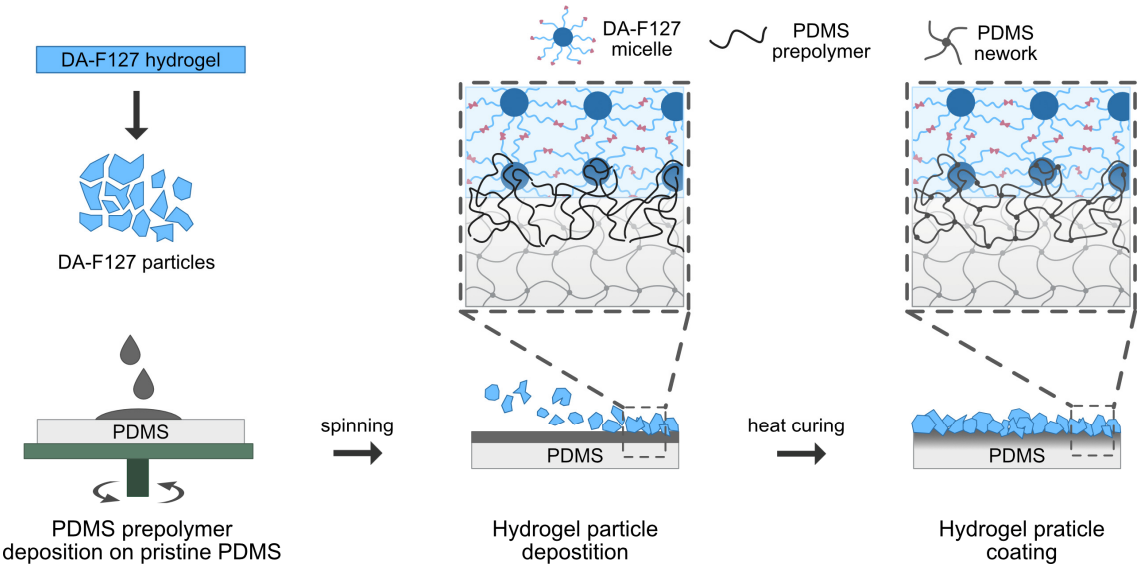

Figure 5. Production scheme of the hydrogel microparticle coating onto PDMS by establishing an interpenetrating polymer network between the PDMS and DA-F127 hydrogel.

To produce PDMS blends developed in Paper 2, different DA-F127–PDMS–H_2O concentrations were mixed and polymerized via a two-step heat and photocuring

process. The as-prepared materials were qualitatively assessed based on visual properties (optical transparency, macroscopic homogeneity, phase separation, and mechanical robustness) and a ternary phase diagram was constructed (**Figure 6A**). Depending on the blend composition a variety of properties were observed ranging from tough and transparent homogeneous materials to fully opaque and macroscopically phase separated mixtures of poor mechanical stability. A representative example of the blend composition effect on the material turbidity can be seen in **Figure 6B**. From here a phase diagram region forming optically transparent and mechanically robust materials was identified. Three compositions B, D and H were chosen for further analysis composed of DA-F127–PDMS–H_2O at a concentration of 40–15–45% w/w, 40–25–35% w/w and 20–60–20% w/w, respectively. While compositions B and D were interesting for evaluation of the effect of relatively low PDMS concentration in the blend, composition H with relatively high PDMS content was deemed especially relevant due to its similarity in mechanics to pristine PDMS.

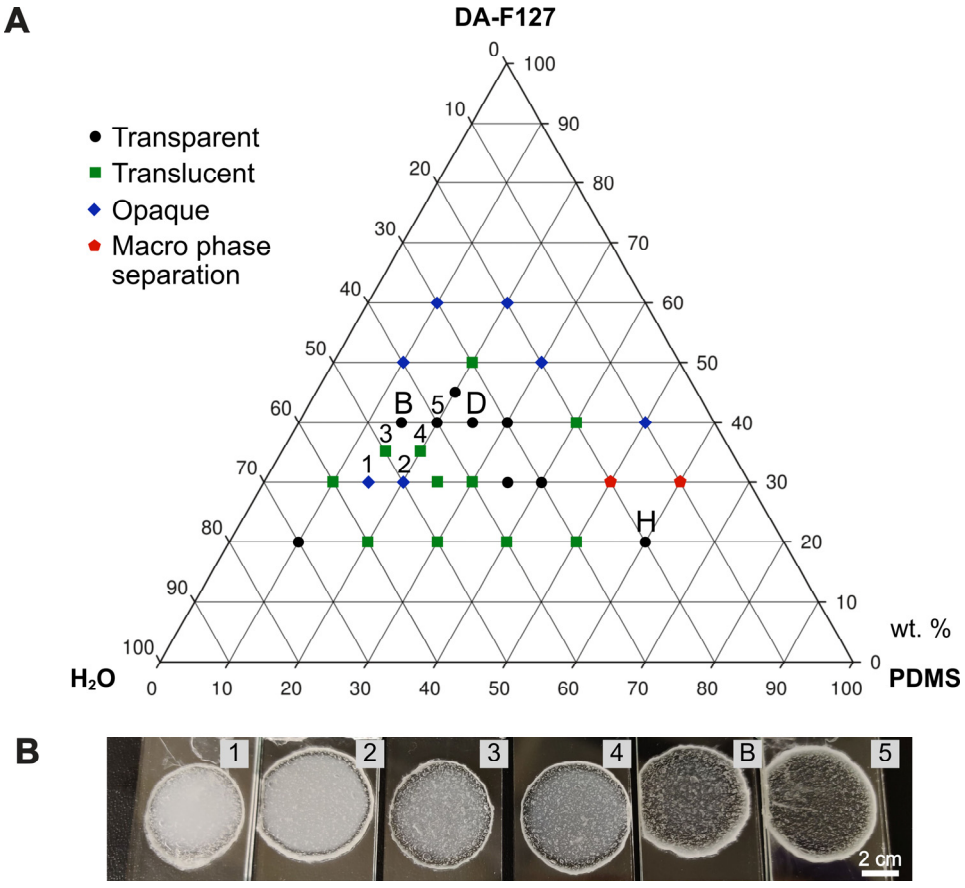

Figure 6. (A) Phase diagram of the synthesized DA-F127–PDMS–H_2O blends and their visual properties based on the composition concentration. Compositions B (40–15–45% w/w), D (40–25–35% w/w) and H (20–60–20% w/w) selected for further evaluation. (B) Composition concentration effect on the material turbidity on selected blends.

4.2. Material characterization

4.2.1. Physicochemical characterization of the materials

The as-prepared hydrogel particle coating developed in Paper 1 was evaluated for the particle size distribution and the adhesion strength. The particle size distribution was measured from stereomicroscopy images and can be seen in **Figure 7A**, with the immobilized particles ranging between 100 to 750 µm in size indicating a broad size distribution. In the case of uniform surface coverage, broad size distribution may be considered beneficial due to denser surface coverage upon particle deposition.

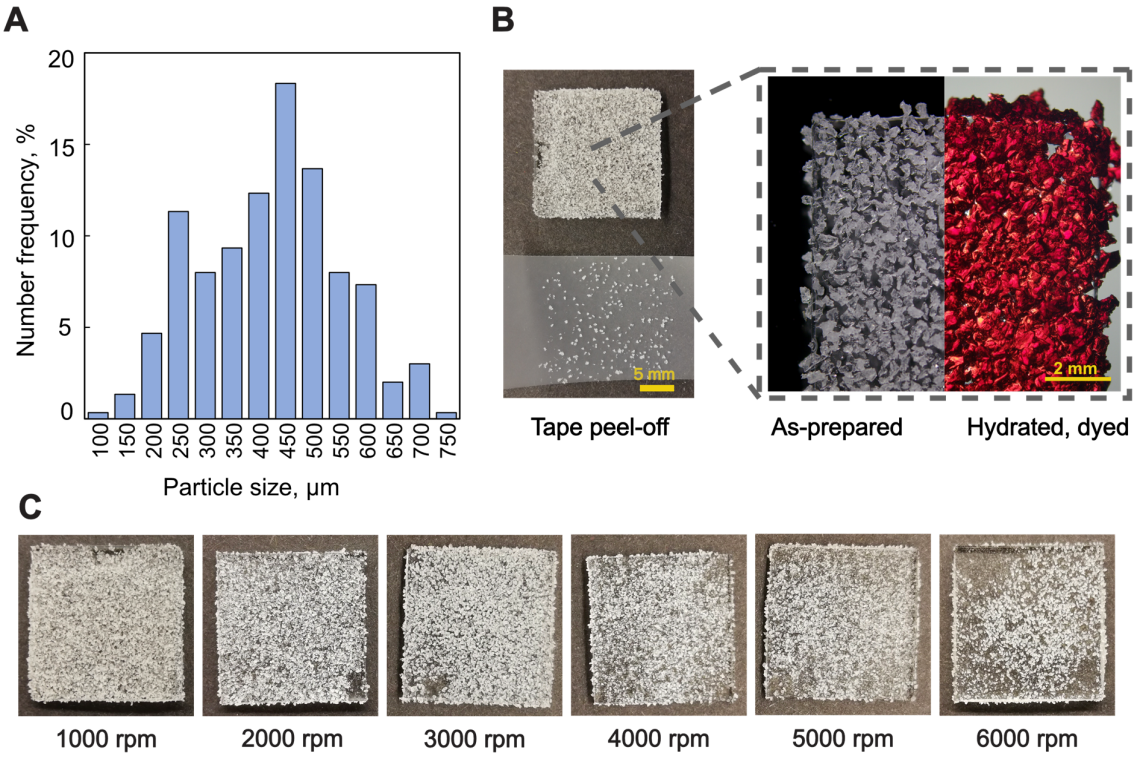

Figure 7. (A) Particle size distribution as measured from as-prepared particle coating. (B) Image of the as-prepared coating made at 3000 rpm with an example of the tape peel-off test and a stereomicroscopy image of the as-prepared coating and safranin hydrated coating demonstrating PDMS coverage. (C) Tape peel-off test on as-prepared coatings made at different spin coating speeds.

To qualitatively evaluate the produced particle coating surface coverage in rehydrated state, coatings were swollen in aqueous safranine dye solution. As evident from **Figure 7B**, hydrogel particles were able to swell without detachment from substrate, fully covering the PDMS substrate. DA-F127 hydrogels are known to be able to swell in water retaining their stability with up to 90% water uptake. The stability of particle

coating in hydrated state is of special importance due to its potential application in close contact with various physiological fluids.

To qualitatively estimated the adhesion strength of particle coatings, Scotch tape peel-off tests were performed on coatings produced at various PDMS film spin rates (**Figure 7C**) [55, 56]. Peel-off test was deemed as a simple and reproducible method to assess the spin coating speed effect on the coating stability and IPN formation between the particles and PDMS. Four consecutive tape applications and removals were performed with the effect on the coating stability evident. Up to 3000 rpm coatings retained their stability with minimal particle detachment by the tape. Following increase in the spin coating speed resulted in consequent increase in the particle detachment, with significant sections of the coating being detached at spin rates above 5000 rpm. These observations serve as a reliable indicator to the spin coating parameters and its effect on coating stability.

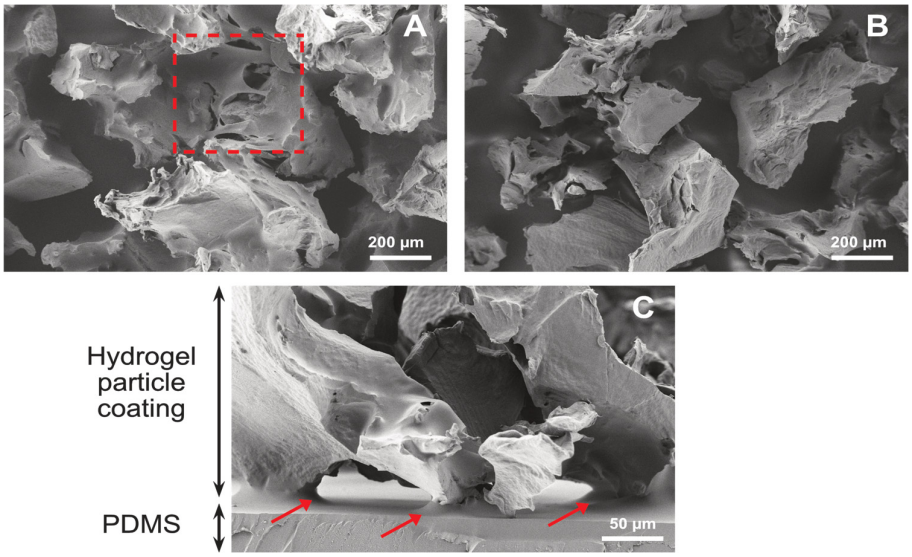

Figure 8. SEM images of coatings produced at different PDMS film spin coating rates. (A) coating produced at 1000 rpm, top view. (B) coating produced at 5000 rpm, top view. (C) coating produced at 5000 rpm, cross-section. PDMS coverage and necking around the particle highlighted with red arrows.

To further investigate the particle adhesion to the PDMS substrates, as-prepared samples produced at different spin coating speeds were imaged with SEM (**Figure 8**). As can be observed in **Figure 8A** coatings prepared at 1000 rpm showed signs of PDMS film covering the underlying particle layer. By increasing the spin coating speed to 3000 rpm and above, PDMS coverage of particles could be avoided, as evident from **Figure 8B**. Although high spin rates proved to be favourable for increased adhesion strength, as seen from tape peel-off test, PDMS coverage can be a potential issue for AMP functionality. Increase in spin rate can therefore be believed to be beneficial, with

increased surface availability resulting in potentially higher contact killing antibacterial effect. Additionally, as seen in **Figure 8C** even at high spin speed of 5000 rpm necking around the particle base can be evident, signifying the PDMS uptake and IPN formation. Put together, tape peel-off test and SEM analysis demonstrate that by carefully tailoring the spin coating speed, hydrogel particle coatings of varying stability can be produced.

To examine the microstructural features of the PDMS blends produced in Paper 2, SEM imaging of the sample cross-sections was performed with the obtained micrographs seen in **Figure 9**. Depending on the composition concentration, notable differences in the synthesized blend microstructure could be observed. Composition B displayed highly microporous architecture characteristic of lyotropic liquid crystals, which can be expected considering the high DA-F127 and water content in the sample. On the contrary, compositions D and H displayed a more homogenous morphology with increased density characteristic of polymer blends. A thread-like morphology could be attributed to composition D, similar to miscible blends, whilst H displayed characteristics of immiscible polymer blends with microphase separation seen throughout the material structure. This observation points towards DA-F127 as the dispersed phase, forming microdomains in the continuous PDMS phase. Overall, the SEM images demonstrate the morphological variation that was achieved by varying of the component concentration in the synthesized PDMS blends.

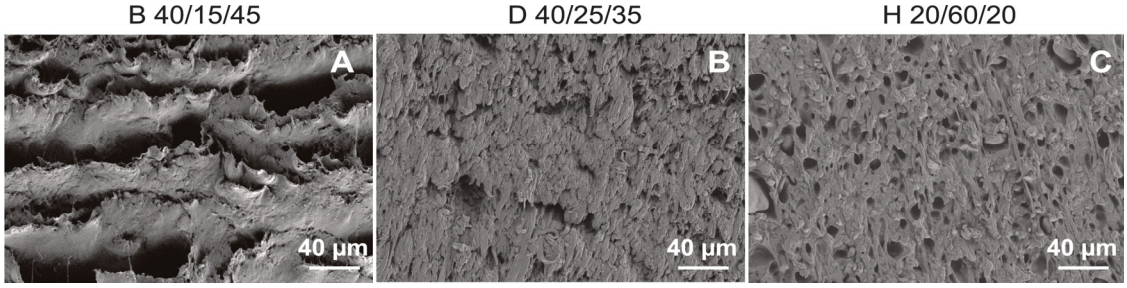

Figure 9. SEM images of the as-prepared PDMS blend microstructures of varying DA-F127–PDMS–H_2O concentration. (A) Blend composition B (40–15–45% w/w), (B) blend composition D (40–25–35% w/w), (C) blend composition H (20–60–20% w/w)

Water contact analysis was performed on the as-prepared PDMS blends developed in Paper 2 to assess the chemical composition effect on the surface wetting characteristics (**Figure 10**). The synthesized compositions were compared to pristine PDMS and 30% w/w DA-F127 hydrogel. Both PDMS and DA-F127 displayed wetting patterns characteristic of the hydrophobic PDMS surface and amphiphilic hydrogel surface, respectively, with the latter displaying WCA reduction because of the hydrogel swelling. All PDMS blends displayed initial WCA surpassing that of pristine PDMS. Generally, compositions B and D had slower wetting characteristics than all other test samples with high initial WCA and continuous reduction, which is partially unexpected

result considering the high DA-F127 and water content in these samples. Additionally, a more rapid initial WCA reduction could be seen for composition H reaching a plateau thereafter. These observations point toward potential discrepancies between the bulk and surface chemical properties, as well as potential surface roughness due to the varied blend microstructures.

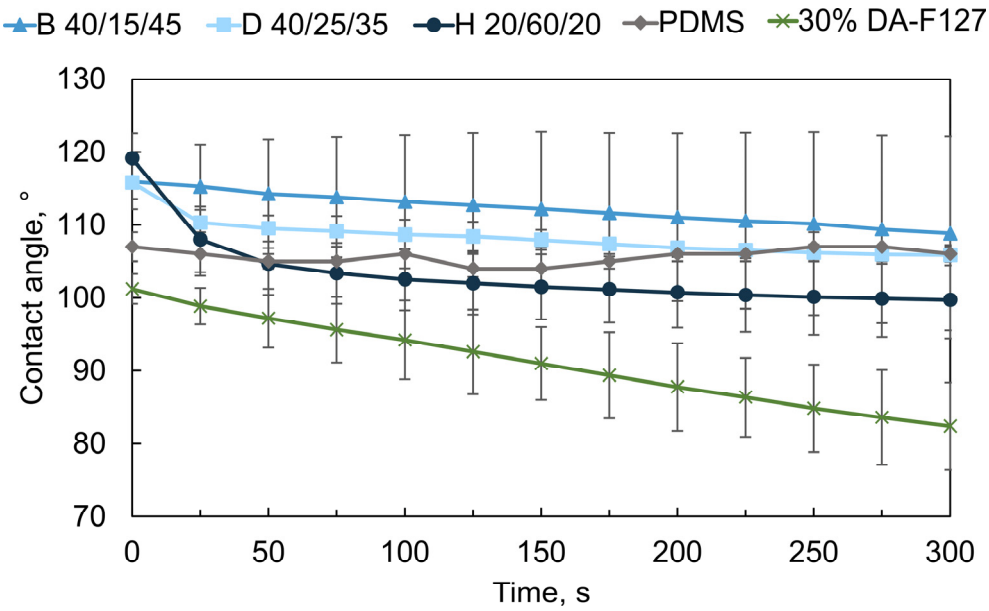

Figure 10. Water contact angle analysis of the as-prepared PDMS blends of varying DA-F127–PDMS–H_2O concentration, pristine PDMS and 30% w/w DA-F127 hydrogel. Blend composition B (40–15–45% w/w), blend composition D (40–25–35% w/w), blend composition H (20–60–20% w/w).

4.2.1.1. AMP functionalization of particle coating

To demonstrate successful AMP functionalization of the AMP particle coating developed in Paper 1, UV-Vis spectroscopy was performed on the AMP functionalized particles prior the immobilization onto PDMS substrates. AMP content was estimated to be around 3.3% w/w with respect to the dry particle mass, indicative of AMP incorporation in the particle structure.

Water contact angle analysis was used as an indirect method to demonstrate AMP presence in the as-prepared AMP particle coating developed Paper 1. **Figure 11** demonstrates the changes in surface wetting properties over time on the dry coatings. Both control and AMP particle coatings demonstrate reduction in WCA as a direct result of the DA-F127 hydrogel network swelling and water uptake. Furthermore, AMP incorporation in the particle coating resulted in marked increase in the wetting time with approximately three times longer wetting period compared to control particle coating. Considering the amphiphilicity of the AMP and the presence of the hydrophobic

tryptophan end tag, the reduction in the wetting rate can be seen as an indirect proof of AMP presence in the particle coating.

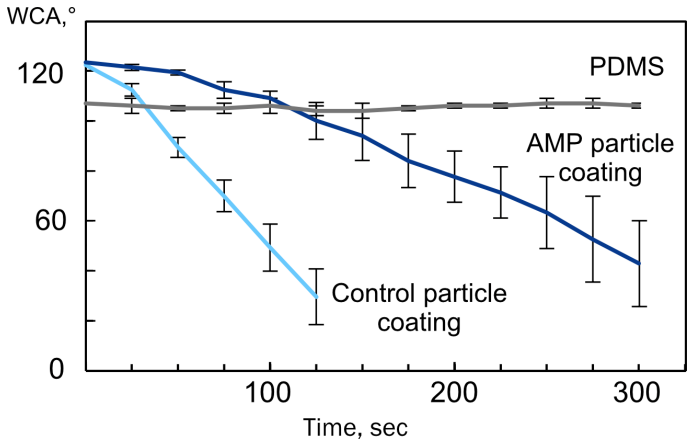

Figure 11. Water contact angle reduction due to swelling of the a-prepared control particle coating, AMP particle coating and pristine PDMS substrates. AMP presence resulting in the reduction of the wetting rate.

Raman spectroscopy was utilized to confirm AMP presence in the AMP particle coating developed in Paper 1. A comparison with the control particle coating was made and the pure AMP powder was used as the reference. As seen from the Raman spectra in **Figure 12,** three characteristic absorption bands present in the pure AMP sample can be seen as small bumps in AMP particle coating sample at 760 cm^{-1}, 1015 cm^{-1} and 1552 cm^{-1}. All three signals can be directly connected to molecular features present in the tryptophan end tag of the AMP molecule. Absorption bands at 760 cm^{-1} and 1015 cm^{-1} can be ascribed to the breathing vibrations of benzene and pyrrole ring originating from the indole ring present in the tryptophan [57, 58]. Similarly, the 1552 cm^{-1} absorption band can be ascribed to the indole ring signal with stretching vibration of benzene and pyrrole rings. These results serve as a more definitive proof of the AMP incorporation in the AMP particle coating structure, however no conclusion as to the covalent attachment mechanism can be drawn here, due to the relatively small concentration of the peptide bonds formed in relation to the abundant polymer background.

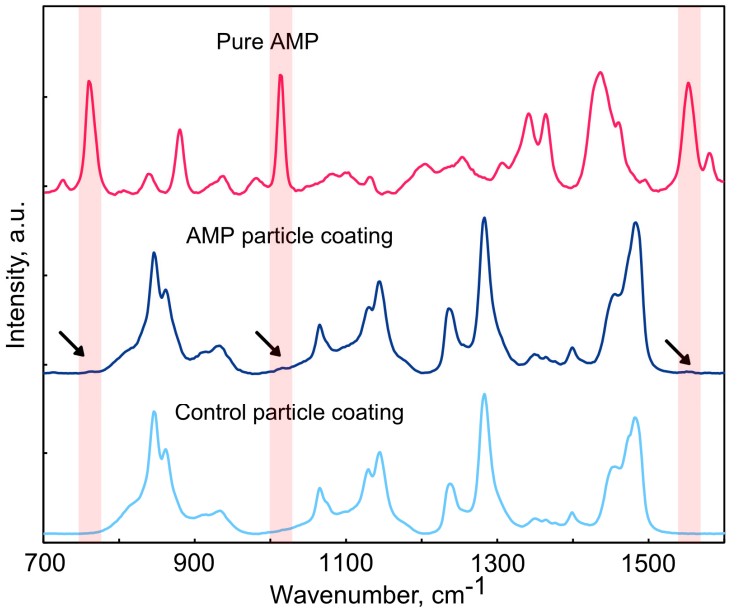

Figure 12. Raman spectra of control particle coating, AMP particle coating and pure AMP. Black arrows indicate absorption bands characteristic of AMP, indicating AMP presence in the AMP particle coating.

For additional characterization of the AMP particle coating developed in Paper 1, XPS was utilized. The survey scans and high-resolution scans of the nitrogen region can be seen in **Figure 13** with the elemental composition seen in **Table 1**. Upon introduction of the AMP particles in the particle coating, appearance of the nitrogen (N 1s) signal could be observed, while absent in control particle coating with the corresponding concentration of 0.2 at.%. This is a strong indicator towards AMP integration into the particle structure via covalent attachment of AMP molecules present on the particle surface. Considering the low analysis depth of XPS (5 – 10 nm) it is probable that the AMP molecules were at the particle surface in the as-prepared state. Additionally, as expected from the particle production, hydrogel particle deposition onto PDMS resulted in increase of the carbon concentration on the control and AMP particle coating samples, originating from the DA-F127 carbon-based backbone.

Overall, the WCA, Raman and XPS results give a good indication towards the integration of AMP molecule into the coating structure. It should be noted that both Raman and XPS utilizes dry samples for analysis, leading to possible peptide reorientation in dry state and reduced signal intensity. Therefore, analysing particle coating activity in swollen state via microbiological analysis is of utmost importance to demonstrate the desired effect of AMP.

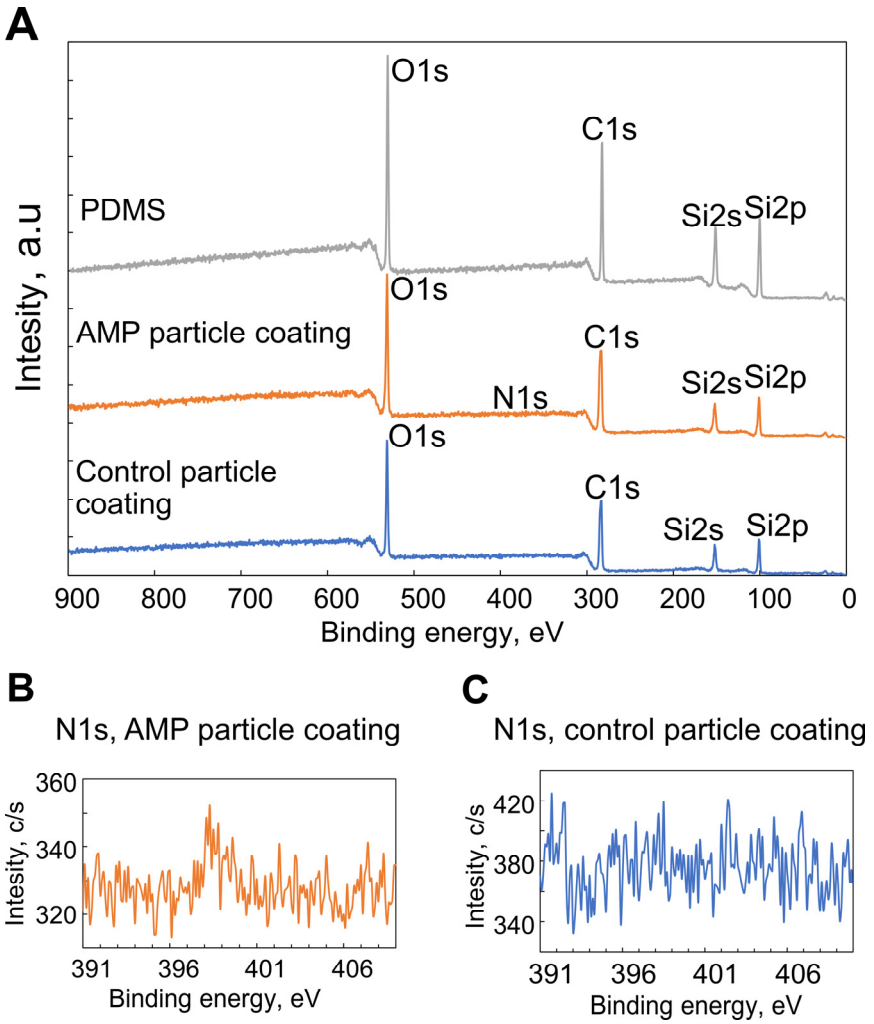

Figure 13. X-ray photoelectron spectroscopy results. (A) XPS survey scans. (B) High resolution scan of N 1s on AMP particle coating. (C) High resolution scan of N 1s on control particle coating.

Table 1. Surface elemental composition of the control particle coating, AMP particle coating and pristine PDMS as determined by XPS.

	Atomic percentage, at.%.			
	C 1s	**O 1s**	**Si 2p**	**N 1s**
PDMS	44.8	31.1	24.1	-
Particle coating	57.2	28.9	13.9	-
AMP particle coating	56.7	29.1	14.0	0.2

4.2.2. Mechanical characterization

Tensile and compression testing was performed on the as-prepared PDMS blends developed in Paper 2 to investigate the composition concentration effect on the blend mechanical properties. The recorded tensile and compressive stress-strain curves can be seen in **Figure 14**. The calculated Young's modulus and compressive moduli as well as determined ultimate tensile and compressive strength are displayed in **Figure 15**. Additionally, pristine PDMS and crosslinked 30% w/w DA-F127 hydrogel samples were included as reference materials.

Compositions B and D displayed similar tensile deformation behaviour to DA-F127 hydrogel with slight increase in strength, stiffness and elasticity, as can be seen from the recorded stress-strain curves and the calculated Young's modulus. Notably different tensile deformation character could be seen in composition H with comparable Young's modulus, but drastic increase in elasticity ($\varepsilon_H \sim 240\%$) – 2 times greater than pristine PDMS elastomer ($\varepsilon_{PDMS} \sim 112\%$) and 3.5 times greater than DA-F127 hydrogel ($\varepsilon_{DA\text{-}F127} \sim 68\%$).

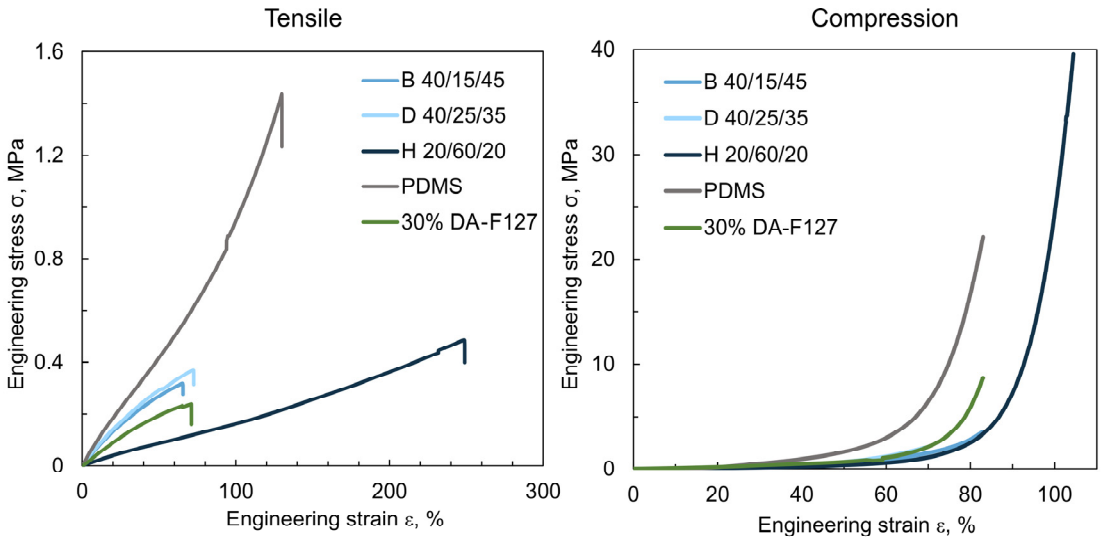

Figure 14. (A) Tensile and (B) compression stress-strain curves of the PDMS blends of varying DA-F127–PDMS–H_2O concentration, pristine PDMS and 30% w/w DA-F127 hydrogel.

The analysis of blends under compression resulted in varying stiffness response depending on the strain with low stiffness seen at low strain, followed by deviation in stiffness upon increased strain. Compositions B and D displayed lower compressive moduli and comparable compressive strength to the DA-F127 hydrogel. In contrast, composition H displayed an increased compressive modulus along with higher compressive strength when compared to both DA-F127 and pristine PDMS.

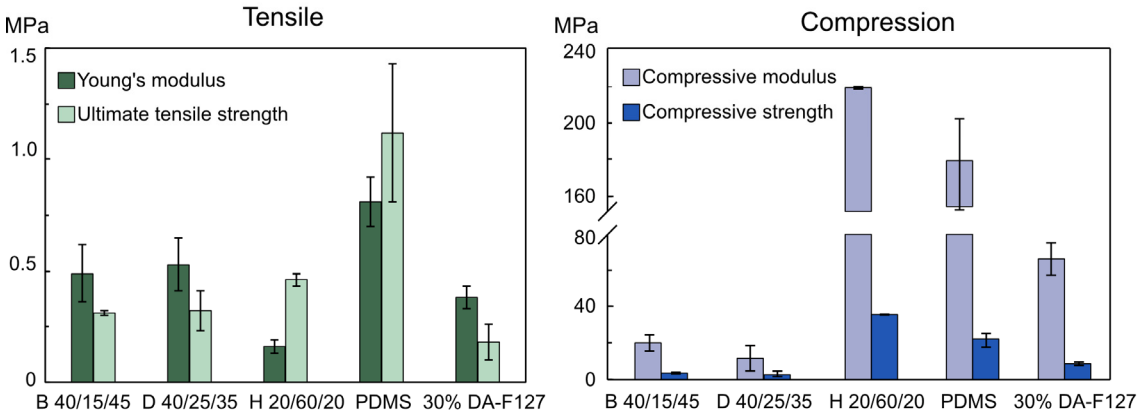

Figure 15. (A) Tensile and (B) compressive parameters calculated from the stress-strain curves of the PDMS blends of varying DA-F127–PDMS–H_2O concentration, pristine PDMS and 30% w/w DA-F127 hydrogel.

A combination of factors could have contributed to the strong deviation in the tensile and compressive behaviour of composition H, such as, material porosity, a reduction in crosslinking density due to increase in polymer chain length, as well as possible nanostructural variations discussed in the following section.

Overall, the mechanical testing results highlight how the variation in DA-F127–PDMS–H_2O ratio in the chosen blend compositions can result in materials with tailored mechanics. By modifying the component concentration, an intermediate rubber-like or hydrogel-like mechanics can be observed, governed by the individual component behaviour.

4.2.3. Material structural characterization

Small-angle X-ray scattering was performed on the PDMS blends developed in Paper 2 to probe for ordered phases in the blend structure. Blend compositions were analysed both in unpolymerized and polymerized state with the recorded SAXS scattering plots seen in **Figure 16**. All unpolymerized compositions displayed a main SAXS peak at q = 0.0426 – 0.0439 $Å^{-1}$ seen in **Figure 16A** that indicate preferential order in the material, most likely from formation of DA-F127 micelles with calculated average micellar dimension of 143 – 147 Å. For compositions B, D and unpolymerized 30% w/w DA-F127 gel two secondary peaks at $q \approx 0.06\ Å^{-1}$ and $q \approx 0.074\ Å^{-1}$ were present corresponding to peak ratio of 1:√4/3:√8/3 that could be ascribed to micellar cubic phase [40]. No secondary peaks could be detected in composition H, suggesting that, although micellar structure was retained, no long-range order was present.

Upon polymerization, loss of secondary peaks could be detected in the SAXS plots for all compositions as seen in **Figure 16B**. Additional changes in the shape and intensity

of the main SAXS peak could be observed, pointing towards increase in the micellar size distribution upon polymerization as evident from the peak broadening. Few reasons could have contributed to the loss of secondary peaks for compositions B and D, namely, random X-ray scattering in a crosslinked material, or loss of order in the system. Similar observations have been reported on crosslinked DA-F127 hydrogels, where micellar cubic phase have been retained after polymerization, however resulting in loss of secondary SAXS peaks [59]. Ultimately, the SAXS results demonstrate how the polymerized PDMS blends retain their micellar structure seen prior polymerization, by forming distorted micellar cubic self-assembled phase throughout the system.

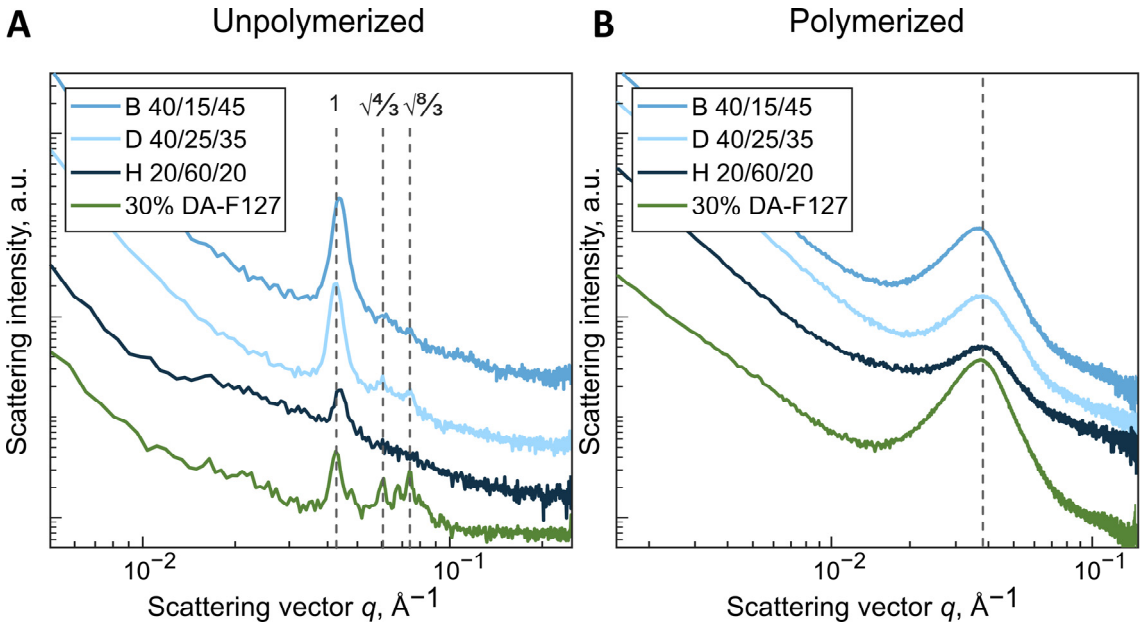

Figure 16. (A) SAXS scattering plot of the blend compositions B, D, H and 30% w/w DA-F127 gel prior polymerization. (B) Synchrotron SAXS scattering plot of polymerized compositions including crosslinked 30% w/w DA-F127 hydrogel. Plots have been shifted vertically for clarity.

4.3. Antibacterial activity of the particle coating

The antibacterial activity of the AMP particle coating developed in Paper 1 can be seen in **Figure 17**. Coating samples were incubated overnight with either *S. epidermidis* or *S. aureus*, followed by bacterial detachment and CFU quantification. The results indicated high antibacterial effect of the AMP particle coating compared to the control particle coating and pristine PDMS substrates for both *S. epidermidis* and *S. aureus.* AMP particle coatings proved to be slightly more effective against *S. epidermidis* resulting in live bacteria reduction by 99.6% (2.4 log, $p < 0.001$) when compared to control coatings and 99.3% (2.1 log, $p < 0.001$) when compared to pristine PDMS. AMP particle coating displayed slightly reduced efficacy against *S. aureus*, whilst remaining

highly active with live bacteria reduction by 94.5% (1.3 log, $p < 0.001$) compared to control coatings and 99.1% (2.1 log, $p < 0.001$) compared to pristine PDMS.

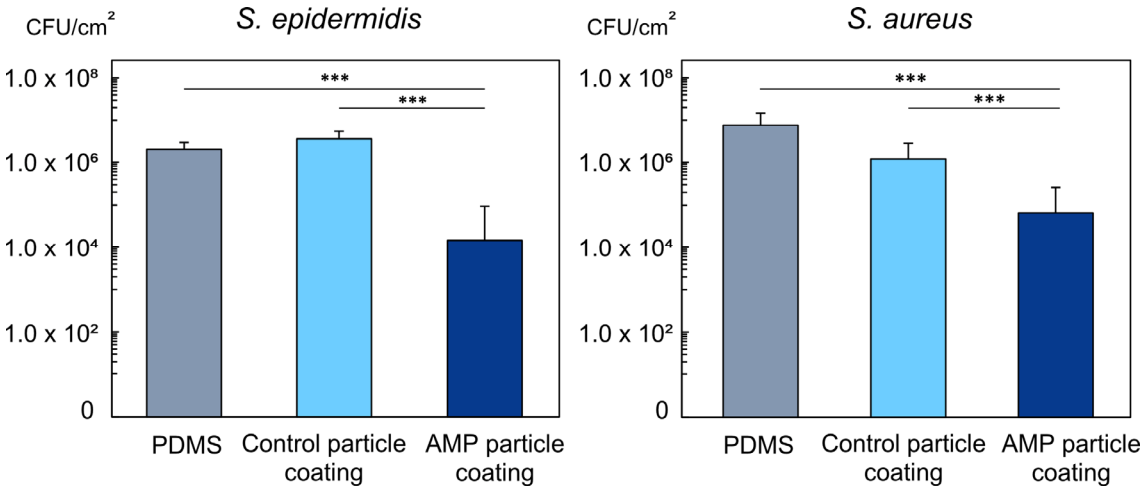

Figure 17. Antibacterial activity of the AMP particle coating against *S. epidermidis* and *S. aureus* from colony counting experiments. CFU/cm^2 calculated from the projected coating surface area. N = 9, *** indicates statistical significance with a p-value of $p \leq 0.001$.

To elucidate the AMP activity mechanisms on the bacterial growth, samples were challenged with increased bacterial concentration (10^8 CFU/ml) of *S. epidermidis* followed by bacteria fixation and SEM analysis. The micrographs of the control and AMP particle coatings after 18 h incubation can be seen in **Figure 18**. It is clear from the images that introduction of AMPs in the particle coating result in stark differences in the bacterial growth behaviour, with significantly higher bacterial load present on the AMP particle coating (**Figure 18C** and **D**) with more dispersed growth characteristic when compared to the control particle coating (**Figure 18A** and **B)**.

While this may seem contradictive to the CFU results, the SEM analysis gives an indication to the electrostatic attraction of the AMP and the bacterial membrane interactions as the basis of the contact killing mechanism. Additionally, considering the increased bacterial concertation used in SEM analysis, direct comparison to the CFU results cannot be drawn, serving more as a qualitative indicator of the AMP effect. Previous studies on DA-F127 hydrogels and hydrogel particles have extensively demonstrated the contact killing potential of covalently immobilized RRP9W4N, further enforcing our findings of AMP particle coating as an effective antibacterial modification strategy of PDMS materials [39, 36].

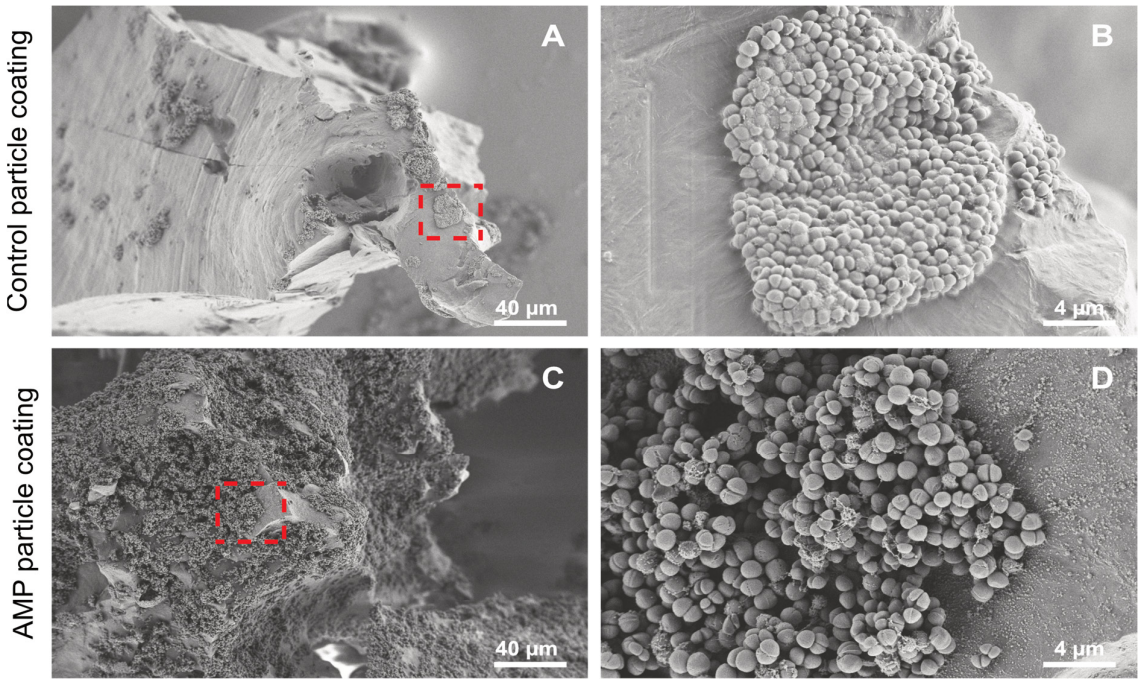

Figure 18. SEM images of (A, B) control particle coating and (C, D) AMP particle coating incubated with *S. epidermidis* for 18 h, demonstrating the AMP electrostatic attraction mechanism of the bacterial cells.

4.4. *In vitro* drug delivery

4.4.1. Drug delivery from the particle coating

To demonstrate an additional functionality of the hydrogel particle coating developed in Paper 1, drug delivery study with VCM, AMP and IBP as the polar, amphiphilic, and nonpolar model drugs, respectively, was carried out. It was believed that by utilizing the polar and nonpolar domains of the DA-F127 hydrogel particle structure, selective drug loading and release could be obtained. The recorded drug release curves can be seen in **Figure 19** with respect to absolute release in milligrams and the estimated cumulative release in percent.

VCM exhibited the most rapid burst release with 60% release achieved in the first 15 min reaching equilibrium in around 2 h. Considering the high polarity and water solubility of VCM, a rapid release patter is to be expected. At a maximum concentration of 0.410 ± 0.073 mg/cm^2 or 0.082 ± 0.015 mg/ml VCM release significantly surpassed MIC for VCM sensitive *S. aureus* (MIC $\leq$ 0.002 mg/ml), indicating loading of therapeutically relevant dose [60].

As to AMP release, a more sustained release pattern was displayed, whilst still retaining an initial burst of around 30% in the first 15 min. Increase in the maximum release

concentration and time could be observed with 1.526 ± 0.168 mg/cm^2 or 0.313 ± 0.040 mg/ml of the drug released in ~ 8 h, owning to the amphiphilic nature of the AMP molecule displaying stronger interactions with the DA-F127 hydrogel particle structure. As in the case with VCM, therapeutically relevant AMP dose was achieved exceeding the MIC up to 20 times (MIC for *S. aureus* ~ 0.012 mg/ml) [36].

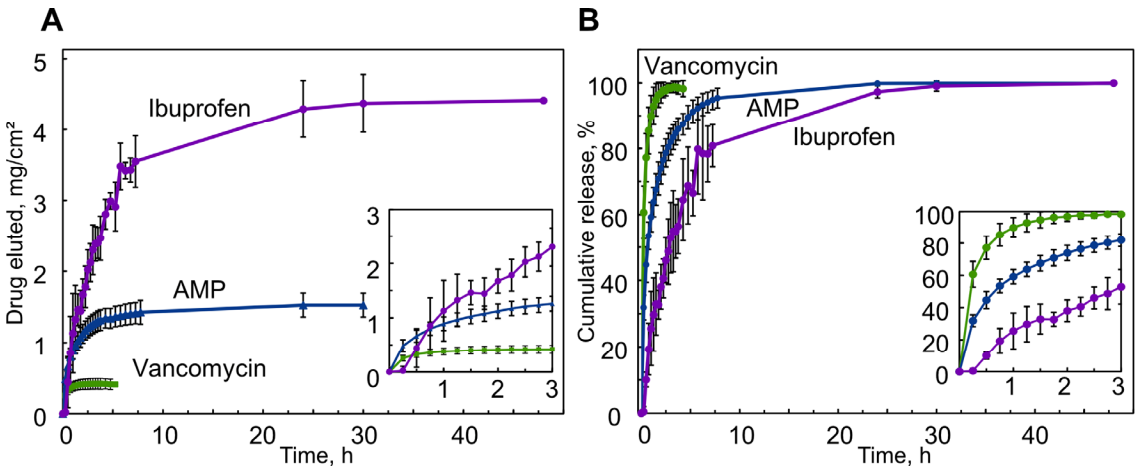

Figure 19. Drug delivery curves of vancomycin, AMP, and ibuprofen release from the control particle coatings. Delivery dose expressed as (A) milligrams of drug eluted per cm^2 of projected coating area, and (B) cumulative release percentage, assuming equilibrium release of 100%, n = 9.

Significantly different IBP release pattern could be observed with maximum concentration 4.373 ± 0.402 mg/cm^2 or 0.331 ± 0.031 mg/ml IBP eluted in ~ 30 h. A few factors are believed to contribute to the drastically different release behaviour of IBP: (1) the hydrophobic interactions of the IBP molecule and the nonpolar domains of the hydrogel, (2) increase in IBP loading solution feed concentration (1% w/v for VCM and AMP, 7% w/v for IBP) and (3) use of SDS as an elution buffer for enhanced solubility.

To further elucidate the drug release mechanism and characterize the kinetics, release data were mathematically fitted to zero order, first order, Korsmeyer-Peppas and Higuchi drug release models as presented in **Table 2**.

VCM displayed the best fit to first order release kinetics with highest correlation coefficient R^2 = 0.992 and lowest RMSE = 1.246 (**Table 3**). First order release kinetics is characterized by concertation-controlled release behaviour and have been previously reported for delivery of highly water soluble drugs from hydrogels [61]. In the case of VCM release from the particle coating, hydrogel network swelling and relaxation, followed by drug diffusion is expected to be the most probable release mechanism [62, 42].

Table 2. Mathematical equations of the drug delivery models used to characterize the release profile of VCM, AMP and IBP from the particle coating.

Kinetic model	**Equation***
Zero order	$Q_t = Q_0 + K_0\, t$
First order	$Q_t = Q_0\, e^{-K_1 t}$
Korsmeyer-Peppas	$\frac{Q_t}{Q_\infty} = K_P\, t^n$
Higuchi	$\frac{Q_t}{Q_\infty} = K_H \sqrt{t}$

* Q_t, Q_0, Q_∞ equals the amount of drug released at time t, initial amount and amount released at equilibrium, respectively. K_0, K_1, K_P, K_H equals the zero order, first order, Korsmeyer-Peppas and Higuchi release constants, respectively. Korsmeyer-Peppas release exponent *n* can be used to characterize the drug release mechanism.

Table 3. Mathematical modelling of the VCM, AMP and IBP delivery data from the particle coating.

Kinetic model	**Vancomycin**				**AMP**				**Ibuprofen**			
	K	***n***	***R²***	**RMSE**	***K***	***n***	***R²***	**RMSE**	***K***	***n***	***R²***	**RMSE**
Zero order	15.660		0.737	6.273	6.635		0.757	8.398	3.856		0.538	16.798
First order	1.777		0.987	1.246	0.447		0.977	2.582	0.241		0.988	2.723
Korsmeyer-Peppas					58.980	0.42	0.991	1.174	22.802	0.73	0.967	3.094
Higuchi	53.690		0.810	5.690	33.800		0.831	7.006	27.140		0.828	10.265

AMP displayed the best fit to Korsmeyer-Peppas model with R^2 = 0.991 and RMSE = 1.174. Korsmeyer-Peppas model is a semi-empirical model, where the exponent *n* can be used to investigate the drug delivery mechanism of unknown delivery systems [63]. In theory, if $n = 0.50$ Fickian diffusion is the governing force for drug delivery via solvent penetration. If $n = 1.0$ the drug delivery is time-independent and limited by polymer relaxation and swelling rate, as in the zero-order model. For $0.50 < n < 1.0$ anomalous transport of simultaneous diffusion and polymer relaxation occurs in a time-dependent manner. For AMP release from the particle coating $n = 0.42$ signifying quasi-Fickian drug release behaviour facilitated by diffusion.

IBP displayed the best fit to the first order release model with R^2 = 0.988 and RMSE = 2.723 with the Korsmeyer-Peppas release exponent n = 0.73, indicating IBP delivery mechanism to be of simultaneous combination of diffusion and polymer chain swelling. With IBP being of low water solubility, its propensity to migrate in the hydrophobic domains of the micellar cubic DA-F127 structure is expected, with the slow swelling of the micelles upon elution as the rate limiting factor in IBP delivery.

Ultimately, with the particle coating exhibiting drastically different release behaviour depending on the drugs' chemical polarity, it can be concluded that the hydrogel particle coating can serve as multifunctional PDMS modification strategy for drug delivery.

4.4.2. Swelling measurements of the PDMS blends

To evaluate the swelling properties of the PDMS blends developed in Paper 2, the as-prepared compositions were swollen in water with the recorded weight changes over time seen in **Figure 20**.

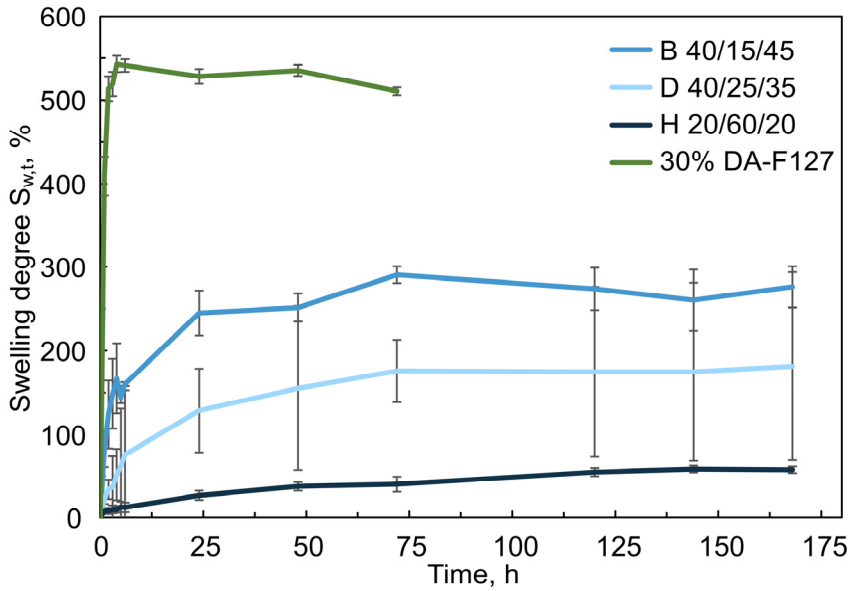

Figure 20. Water swelling measurements of the PDMS blends of varying DA-F127–PDMS–H_2O concentration and 30% w/w DA-F127 hydrogel.

All test composition retained their weight for 7 days without any mass loss, indicative of stable crosslinking between the polymer phases. When compared to DA-F127 hydrogel, compositions B, D an H exhibited reduced swelling degree pointing towards increased network crosslinking density in the presence of PDMS. Nonetheless a stable hydration profile could be observed for all compositions with equilibrium swelling degree reached after ~ 72 h, and maximums swelling degree of 270%, 170% and 55% for composition B, D and H, respectively. As expected, DA-F127 hydrogel displayed

significantly higher and rapid hydration reaching maximum swelling after ~ 4 h. The swelling measurements illustrate that by tailoring the PDMS blend composition, large variation in the swelling degree and water uptake can be achieved with special significance in the encapsulation and delivery of drugs discussed in the following section.

4.4.3. Drug delivery from the PDMS blends

To evaluate the drug encapsulation and release properties of the PDMS blends developed in Paper 2, drug delivery studies were performed utilizing VCM and IBP as the polar and nonpolar drugs, respectively. The recorded drug release curves of the different compositions can be seen in **Figure 21**.

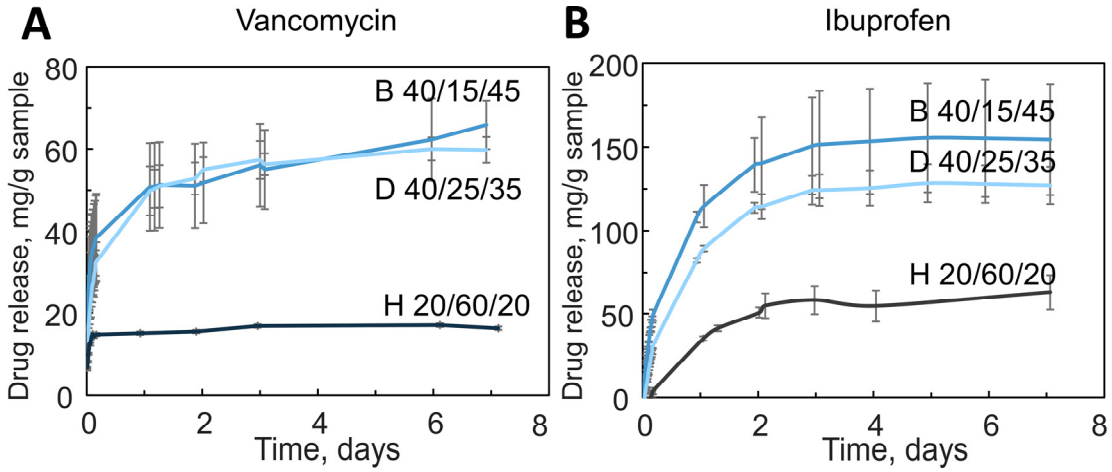

Figure 21. Drug delivery curves of (A) vancomycin and (B) ibuprofen release from the PDMS blends. Delivery dose expressed as the amount of drug released per unit of sample mass.

Similar to the water swelling measurements, compositions B and D displayed the highest dose of drug delivered both for VCM and IBP. For VCM, an initial burst release followed by a sustained release behaviour could be observed for up to 7 and 6 days for B and D, respectively, with very similar profiles generated. For IBP, a gradual profile was displayed with equilibrium dose delivered after ~ 5 days. Here composition B was seen to deliver the highest IBP dose – 17% more than composition D. Considering the high DA-F127 and water content in the compositions B and D increased drug dose can be expected, when compared to the more PDMS rich composition H.

Composition H resulted in the lowest drug dose eluted both for VCM and IBP. VCM profile displayed a minor burst release in the first few hours, with no additional release detected afterwards. Considering the high PDMS and low DA-F127 content, a reduction in the polar drug's initial uptake can be expected, indicating nonuniform distribution of the VCM throughout the material structure, with majority located near the surface. A

sustained delivery profile was observed for IBP release with gradual increase reaching equilibrium after ~ 3 days, indicative of a more uniform distribution of the nonpolar drug. As in the case of IBP delivery from the hydrogel particle coatings discussed previously, all blend compositions displayed increase in the IBP dose delivered compared to VCM due to a combination of factors, namely, (1) use of acetone as the loading buffer facilitating the composition swelling and drug uptake, (2) the hydrophobic interactions of the IBP molecule and the nonpolar domains of the PDMS and DA-F127 structure leading to a more sustained elution, (3) increase in IBP loading solution feed concentration (1% w/v for VCM and AMP, 10% w/v for IBP) and (4) use of SDS as an elution buffer resulting in enhanced solubility.

Overall, results gathered from the drug delivery study demonstrates how the PDMS blends are capable to encapsulate and release both polar and nonpolar drugs in a sustained manner, demonstrating improved functionality of the materials compared to pristine PDMS and DA-F127 hydrogels alone.

4.5. 3D printing of the PDMS blend

As a proof-of-concept of potential medical device, the blend composition B developed in Paper 2 was chosen to demonstrate the material's processing capabilities via extrusion-based 3D printing. **Figure 22** demonstrates how composition B could be successfully employed to print a capillary tube and scaled-down human nose model with high resolution and precision. Upon addition of the DA-F127 in the blend composition, unpolymerized gels acquire rheological properties suitable for 3D printing, displaying shear-induced flow capable of recovering its structural integrity upon removal of the force [64, 59]. This type of behaviour is characteristic of LLC gels like the Pluronic F127, therefore additionally motivating DA-F127 addition in the blend system. The material's ability to be 3D printed offers an improved application potential where customised geometries can be printed for different biomedical applications.

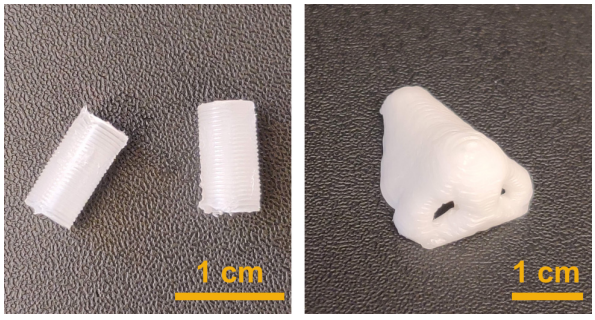

Figure 22. 3D printed capillary tube and scaled-down human nose from lend composition B (40–15–45% w/w).

5. Conclusions

The work presented in this thesis aimed to develop two alternative polydimethylsiloxane (PDMS) modification strategies to produce elastomers with antibacterial and drug-release properties.

The study resulted in successful surface modification of PDMS with an antimicrobial peptide-hydrogel microparticle coating, that enabled contact killing antibacterial effect along with localised drug release feature. The results demonstrated a stable hydrogel particle coating onto PDMS, developed by physically immobilizing hydrogel particles on the PDMS surface via interpenetrating polymer network formation. The physiochemical characterization confirmed PDMS surface modification with hydrophilic properties along with covalent immobilization of AMP. Upon covalent attachment of AMP, the coatings exhibited high antibacterial effect against *S. epidermidis* and *S. aureus* – clinically relevant strains present in medical device-associated infection – which have important implications for infection inhibition. Additionally, sustained drug delivery capacity of polar, amphiphilic, and nonpolar drugs was demonstrated using vancomycin, AMP, and ibuprofen, as the respective model drugs yielding multifunctional PDMS surface properties.

As a second alternative bulk PDMS modification was utilized, resulting in synthesis of novel PDMS-hydrogel blends with localized drug delivery capacity. PDMS and triblock copolymer (diacrylated Pluronic F127) hydrogel blends were prepared exploring various ternary PDMS–DA-F127–H_2O compositions. Three compositions of interest were further investigated, demonstrating tailorable mechanics and water retention capacity along with self-assembled nanostructure. A sustained drug release profile was generated upon encapsulation and release of polar vancomycin and nonpolar ibuprofen drugs, endowing the PDMS elastomer with improved functionalities.

Ultimately, both strategies offer a potential solution for the mitigation of medical device-associated infection via development of antibacterial PDMS materials with a potential application in medical device production.

6. Future perspectives

The current work focused on using hydrogel particles produced by top-down methods, resulting in a wide size distribution. For future work, it would be of interest to investigate the particle size distribution effect on the resulting antibacterial activity by varying the size of immobilized particles with potential improvements in the antibacterial properties. Although in the work so far, particle coatings have been demonstrated to have dual function of antibacterial contact killing effect and drug-eluting properties, it would be interesting to investigate co-administration possibilities for a simultaneous rapid contact killing effect as well as a sustained antibacterial effect. Additionally, antibacterial activity analysis must be carried out on broad spectrum of gram-negative and drug-resistant bacterial strains for a more detailed insight in the antibacterial activity limits generated by the AMP particle coating.

Regarding the PDMS blends, the research has so far focused on using one type of silicone and one type of amphiphile, which offers a strong potential for exploring new material combinations. For further improvement of the blends' stability and functionality, silicones of different molecular weight and functionality could be used, along with Pluronic molecules of modified PEO-PPO block length. Further on, to closer address the objectives of development of antibacterial elastomers, it would be of interest to investigate the direct AMP attachment to the blend surface, to endow the blends with contact killing potential, along with drug-eluting capacity, resulting in multifunctional materials. Ultimately, *in vitro* antibacterial activity of the produced blends ought to be tested against common bacterial strains involved in medical device associated infections.

To facilitate the use of elastomeric materials developed in this thesis for real-life medical device applications, *in vitro* cytotoxicity assays need to be carried out on the developed materials, to evaluate cell-material interactions from a biocompatibility point of view and identify any potential toxic effects. Additionally, to give a more realistic view on how these materials would perform *in vivo*, an *in vivo* antibacterial activity tests can be performed on an animal infection models.

7. References

[1] P. S. Stewart and T. Bjarnsholt, "Risk factors for chronic biofilm-related infection associated with implanted medical devices," *Clin. Microbiol. Infect.*, vol. 26, no. 8, pp. 1034–1038, Aug. 2020, doi: 10.1016/j.cmi.2020.02.027.

[2] L. E. Nicolle, "Catheter associated urinary tract infections," *Antimicrob. Resist. Infect. Control*, vol. 3, no. 1, p. 23, Dec. 2014, doi: 10.1186/2047-2994-3-23.

[3] R. M. Donlan, "Biofilms: Microbial Life on Surfaces," *Emerg. Infect. Dis.*, vol. 8, no. 9, pp. 881–890, Sep. 2002, doi: 10.3201/eid0809.020063.

[4] C. J. Murray *et al.*, "Global burden of bacterial antimicrobial resistance in 2019: a systematic analysis," *Lancet*, vol. 399, no. 10325, pp. 629–655, Feb. 2022, doi: 10.1016/S0140-6736(21)02724-0.

[5] L. M. Weiner-Lastinger MPH *et al.*, "Antimicrobial-resistant pathogens associated with adult healthcare-associated infections: Summary of data reported to the National Healthcare Safety Network, 2015–2017," *Infect. Control Hosp. Epidemiol.*, vol. 41, no. 1, pp. 1–18, Jan. 2020, doi: 10.1017/ICE.2019.296.

[6] C. Zhao, L. Zhou, M. Chiao, and W. Yang, "Antibacterial hydrogel coating: Strategies in surface chemistry," *Adv. Colloid Interface Sci.*, vol. 285, p. 102280, Nov. 2020, doi: 10.1016/j.cis.2020.102280.

[7] M. Zare, E. R. Ghomi, P. D. Venkatraman, and S. Ramakrishna, "Silicone-based biomaterials for biomedical applications: Antimicrobial strategies and 3D printing technologies," *J. Appl. Polym. Sci.*, vol. 138, no. 38, p. 50969, Oct. 2021, doi: 10.1002/app.50969.

[8] R. Yoda, "Elastomers for biomedical applications," *J. Biomater. Sci. Polym. Ed.*, vol. 9, no. 6, pp. 561–626, 1998, doi: 10.1163/156856298X00046.

[9] M. Navarro, A. Michiardi, O. Castaño, and J. . Planell, "Biomaterials in orthopaedics," *J. R. Soc. Interface*, vol. 5, no. 27, pp. 1137–1158, Oct. 2008, doi: 10.1098/rsif.2008.0151.

[10] D. Spiller *et al.*, "PDMS content affects in vitro hemocompatibility of synthetic vascular grafts," *J. Mater. Sci. Mater. Med.*, vol. 18, no. 6, pp. 1097–1104, Jun. 2007, doi: 10.1007/s10856-006-0067-0.

[11] S. Chen, L. Li, C. Zhao, and J. Zheng, "Surface hydration: Principles and applications toward low-fouling/nonfouling biomaterials," *Polymer (Guildf).*, vol. 51, no. 23, pp. 5283–5293, Oct. 2010, doi: 10.1016/j.polymer.2010.08.022.

[12] D. M. Siddiq and R. O. Darouiche, "New strategies to prevent catheter-associated urinary tract infections," *Nat. Rev. Urol.*, vol. 9, no. 6, pp. 305–314, 2012, doi: 10.1038/nrurol.2012.68.

[13] N. Shen *et al.*, "Photograftable zwitterionic coatings prevent staphylococcus aureus and staphylococcus epidermidis adhesion to PDMS surfaces," *ACS Appl. Bio Mater.*, vol. 2021, pp. 1283–1293, Feb. 2021, doi: 10.1021/acsabm.0c01147.

[14] A. Zhang, L. Cheng, S. Hong, C. Yang, and Y. Lin, "Preparation of anti-fouling silicone elastomers by covalent immobilization of carboxybetaine," *RSC Adv.*, vol. 5, no. 107, pp. 88456–88463, 2015, doi: 10.1039/c5ra17206c.

[15] S. B. Yeh, C. S. Chen, W. Y. Chen, and C. J. Huang, "Modification of silicone elastomer with zwitterionic silane for durable antifouling properties," *Langmuir*, vol. 30, no. 38, pp. 11386–11393, Sep. 2014, doi: 10.1021/la502486e.

[16] S. Wu, B. Zhang, Y. Liu, X. Suo, and H. Li, "Influence of surface topography on bacterial adhesion: A review (Review)," *Biointerphases*, vol. 13, no. 6, p. 060801, Dec. 2018, doi: 10.1116/1.5054057.

[17] S. Hou, H. Gu, C. Smith, and D. Ren, "Microtopographic patterns affect escherichia coli biofilm formation on poly(dimethylsiloxane) surfaces," *Langmuir*, vol. 27, no. 6, pp. 2686–2691, Mar. 2011, doi: 10.1021/la1046194.

[18] L. E. Fisher *et al.*, "Biomaterial modification of urinary catheters with antimicrobials to give long-term broadspectrum antibiofilm activity," *J. Control. Release*, vol. 202, pp. 57–64, 2015, doi: 10.1016/j.jconrel.2015.01.037.

[19] K. Belfield, X. Chen, E. F. Smith, W. Ashraf, and R. Bayston, "An antimicrobial impregnated urinary catheter that reduces mineral encrustation and prevents colonisation by multi-drug resistant organisms for up to 12 weeks," *Acta Biomater.*, vol. 90, pp. 157–168, May 2019, doi: 10.1016/j.actbio.2019.03.042.

[20] D. Campoccia, L. Montanaro, and C. R. Arciola, "A review of the biomaterials technologies for infection-resistant surfaces," *Biomaterials*, vol. 34, no. 34, pp. 8533–8554, Nov. 2013, doi: 10.1016/j.biomaterials.2013.07.089.

[21] P. Singha, J. Locklin, and H. Handa, "A review of the recent advances in antimicrobial coatings for urinary catheters," *Acta Biomater.*, vol. 50, pp. 20–40, 2017, doi: 10.1016/j.actbio.2016.11.070.

[22] R. Pickard *et al.*, "Antimicrobial catheters for reduction of symptomatic urinary tract infection in adults requiring short-term catheterisation in hospital: A multicentre randomised controlled trial," *Lancet*, vol. 380, no. 9857, pp. 1927–1935, 2012, doi: 10.1016/S0140-6736(12)61380-4.

[23] P. Jahn, K. Beutner, and G. Langer, "Types of indwelling urinary catheters for long-term bladder drainage in adults," *Cochrane Database Syst. Rev.*, no. 10, Oct. 2012, doi: 10.1002/14651858.CD004997.pub3.

[24] L. Ferreira and A. Zumbuehl, "Non-leaching surfaces capable of killing microorganisms on contact," *J. Mater. Chem.*, vol. 19, no. 42, p. 7796, 2009, doi: 10.1039/b905668h.

[25] M. Bračič, O. Šauperl, S. Strnad, I. Kosalec, O. Plohl, and L. F. Zemljič, "Surface modification of silicone with colloidal polysaccharides formulations for the development of antimicrobial urethral catheters," *Appl. Surf. Sci.*, vol. 463, pp. 889–899, Jan. 2019, doi: 10.1016/j.apsusc.2018.09.015.

[26] R. Wang, K. G. Neoh, Z. Shi, E. T. Kang, P. A. Tambyah, and E. Chiong, "Inhibition of escherichia coli and proteus mirabilis adhesion and biofilm formation on medical grade silicone surface," *Biotechnol. Bioeng.*, vol. 109, no. 2, pp. 336–345, Feb. 2012, doi: 10.1002/bit.23342.

[27] J. J. Dong, A. Muszanska, F. Xiang, R. Falkenberg, B. Van De Belt-Gritter, and T. Loontjens, "Contact Killing of Gram-Positive and Gram-Negative Bacteria on PDMS Provided with Immobilized Hyperbranched Antibacterial Coatings," *Langmuir*, vol. 35, no. 43, pp. 14108–14116, Oct. 2019, doi: 10.1021/acs.langmuir.9b02549.

[28] K. Lim, R. R. Y. Chua, B. Ho, P. A. Tambyah, K. Hadinoto, and S. S. J. Leong, "Development of a catheter functionalized by a polydopamine peptide coating with antimicrobial and antibiofilm properties," *Acta Biomater.*, vol. 15, pp. 127–138, Mar. 2015, doi: 10.1016/j.actbio.2014.12.015.

[29] K. Lim *et al.*, "Immobilization studies of an engineered arginine-tryptophan-rich peptide on a silicone surface with antimicrobial and antibiofilm activity," *ACS Appl. Mater. Interfaces*, vol. 5, no. 13, pp. 6412–6422, Jul. 2013, doi: 10.1021/am401629p.

[30] B. Mishra *et al.*, "Site specific immobilization of a potent antimicrobial peptide onto silicone catheters: evaluation against urinary tract infection pathogens," *J. Mater. Chem. B*, vol. 2, no. 12, p. 1706, 2014, doi: 10.1039/c3tb21300e.

[31] M. Zasloff, "Antimicrobial peptides of multicellular organisms," *Nature*, vol. 415, no. 6870, pp. 389–395, Jan. 2002, doi: 10.1038/415389a.

[32] K. Lim and S. S. J. Leong, "Antimicrobial Coating Development Based on Antimicrobial Peptides," in *Handbook of Antimicrobial Coatings*, Elsevier, 2018, pp. 509–532.

[33] A. A. Bahar and D. Ren, "Antimicrobial peptides.," *Pharmaceuticals (Basel).*, vol. 6, no. 12, pp. 1543–75, Nov. 2013, doi: 10.3390/ph6121543.

[34] A. T. Y. Yeung, S. L. Gellatly, and R. E. W. Hancock, "Multifunctional cationic host defence peptides and their clinical applications," *Cell. Mol. Life Sci.*, vol. 68, no. 13, pp. 2161–2176, 2011, doi: 10.1007/s00018-011-0710-x.

[35] M. Malmsten, G. Kasetty, M. Pasupuleti, J. Alenfall, and A. Schmidtchen, "Highly Selective End-Tagged Antimicrobial Peptides Derived from PRELP," *PLoS One*, vol. 6, no. 1, p. e16400, Jan. 2011, doi: 10.1371/journal.pone.0016400.

[36] E. Blomstrand, A. K. Rajasekharan, S. Atefyekta, and M. Andersson, "Cross-linked lyotropic liquid crystal particles functionalized with antimicrobial peptides," *Int. J. Pharm.*, vol. 627, p. 122215, Nov. 2022, doi: 10.1016/j.ijpharm.2022.122215.

[37] F. Costa, I. F. Carvalho, R. C. Montelaro, P. Gomes, and M. C. L. Martins, "Covalent immobilization of antimicrobial peptides (AMPs) onto biomaterial surfaces," *Acta Biomater.*, vol. 7, no. 4, pp. 1431–1440, 2011, doi: 10.1016/j.actbio.2010.11.005.

[38] S. A. Onaizi and S. S. J. Leong, "Tethering antimicrobial peptides: Current status and potential challenges," *Biotechnology Advances*, vol. 29, no. 1. Elsevier, pp. 67–74, 01-Jan-2011, doi: 10.1016/j.biotechadv.2010.08.012.

[39] S. Atefyekta *et al.*, "Antimicrobial Peptide-Functionalized Mesoporous Hydrogels," *ACS Biomater. Sci. Eng.*, vol. 7, no. 4, pp. 1693–1702, Apr. 2021, doi: 10.1021/acsbiomaterials.1c00029.

[40] P. Holmqvist, P. Alexandridis, and B. Lindman, "Modification of the Microstructure in Block Copolymer−Water−'Oil' Systems by Varying the Copolymer Composition and the 'Oil' Type: Small-Angle X-ray Scattering and Deuterium-NMR Investigation," *J. Phys. Chem. B*, vol. 102, no. 7, pp. 1149–1158, 1998, doi: 10.1021/jp9730297.

[41] S. Nie, W. W. Hsiao, W. Pan, and Z. Yang, "Thermoreversible pluronic® F127-based hydrogel containing liposomes for the controlled delivery of paclitaxel: In vitro drug release, cell cytotoxicity, and uptake studies," *Int. J. Nanomedicine*, vol. 6, no. 1, pp. 151–166, 2011, doi: 10.2147/IJN.S15057.

[42] M. L. Veyries *et al.*, "Controlled release of vancomycin from Poloxamer 407 gels," *Int. J. Pharm.*, vol. 192, no. 2, pp. 183–193, Dec. 1999, doi: 10.1016/S0378-5173(99)00307-5.

[43] H. Almeida *et al.*, "Preparation, characterization and biocompatibility studies of thermoresponsive eyedrops based on the combination of nanostructured lipid carriers (NLC) and the polymer Pluronic F-127 for controlled delivery of ibuprofen," *Pharm. Dev. Technol.*, vol. 22, no. 3, pp. 336–349, 2017, doi: 10.3109/10837450.2015.1125922.

[44] J. C. Quarterman, S. M. Geary, and A. K. Salem, "Evolution of drug-eluting biomedical implants for sustained drug delivery," *Eur. J. Pharm. Biopharm.*, vol. 159, pp. 21–35, Feb. 2021, doi: 10.1016/j.ejpb.2020.12.005.

[45] D. Campoccia, L. Montanaro, P. Speziale, and C. R. Arciola, "Antibiotic-loaded biomaterials and the risks for the spread of antibiotic resistance following their prophylactic and therapeutic clinical use," *Biomaterials*, vol. 31, no. 25, pp. 6363–6377, Sep. 2010, doi: 10.1016/j.biomaterials.2010.05.005.

[46] Y. Qin, "Applications of advanced technologies in the development of functional

medical textile materials," in *Medical Textile Materials*, Elsevier, 2016, pp. 55–70.

[47] F. S. BATES, "Polymer-Polymer Phase Behavior," *Science (80-.).*, vol. 251, no. 4996, pp. 898–905, Feb. 1991, doi: 10.1126/science.251.4996.898.

[48] A. Abdilla *et al.*, "Silicone-based polymer blends: Enhancing properties through compatibilization," *J. Polym. Sci.*, vol. 59, no. 19, pp. 2114–2128, Oct. 2021, doi: 10.1002/pol.20210453.

[49] P. Lucas and J.-J. Robin, "Silicone-Based Polymer Blends: An Overview of the Materials and Processes," in *Functional Materials and Biomaterials*, Berlin, Heidelberg: Springer Berlin Heidelberg, 2007, pp. 111–147.

[50] U. Jorzik and B. A. Wolf, "Reduction of the interfacial tension between poly(dimethylsiloxane) and poly(ethylene oxide) by block copolymers: Effects of molecular architecture and chemical composition," *Macromolecules*, vol. 30, no. 16, pp. 4713–4718, Aug. 1997, doi: 10.1021/ma9613300.

[51] F. Abbasi, H. Mirzadeh, and A. A. Katbab, "Modification of polysiloxane polymers for biomedical applications: A review," *Polym. Int.*, vol. 50, no. 12, pp. 1279–1287, Dec. 2001, doi: 10.1002/pi.783.

[52] M. Gehrke, J. Sircoglou, C. Vincent, J. Siepmann, and F. Siepmann, "How to adjust dexamethasone mobility in silicone matrices: A quantitative treatment," *Eur. J. Pharm. Biopharm.*, vol. 100, pp. 27–37, Mar. 2016, doi: 10.1016/j.ejpb.2015.11.018.

[53] A. I. Panou, K. G. Papadokostaki, and M. Sanopoulou, "Release mechanisms of semipolar solutes from poly(dimethylsiloxane) elastomers: Effect of a hydrophilic additive," *J. Appl. Polym. Sci.*, vol. 131, no. 18, pp. 9381–9388, Sep. 2014, doi: 10.1002/app.40782.

[54] Y. Zhang *et al.*, "DDSolver: An add-in program for modeling and comparison of drug dissolution profiles," *AAPS J.*, vol. 12, no. 3, pp. 263–271, Sep. 2010, doi: 10.1208/s12248-010-9185-1.

[55] R. R. Kisannagar, P. Jha, A. Navalkar, S. K. Maji, and D. Gupta, "Fabrication of Silver Nanowire/Polydimethylsiloxane Dry Electrodes by a Vacuum Filtration Method for Electrophysiological Signal Monitoring," *ACS Omega*, vol. 5, no. 18, pp. 10260–10265, 2020, doi: 10.1021/acsomega.9b03678.

[56] S. W. Lee *et al.*, "Adhesion test of carbon nanotube film coated onto transparent conducting substrates," *Nano*, vol. 5, no. 3, pp. 133–138, Nov. 2010, doi: 10.1142/S1793292010002025.

[57] F. Madzharova, Z. Heiner, and J. Kneipp, "Surface Enhanced Hyper-Raman Scattering of the Amino Acids Tryptophan, Histidine, Phenylalanine, and Tyrosine," *J. Phys. Chem. C*, vol. 121, no. 2, pp. 1235–1242, Jan. 2017, doi:

10.1021/acs.jpcc.6b10905.

[58] G. Zhu, X. Zhu, Q. Fan, and X. Wan, "Raman spectra of amino acids and their aqueous solutions," *Spectrochim. Acta - Part A Mol. Biomol. Spectrosc.*, vol. 78, no. 3, pp. 1187–1195, Mar. 2011, doi: 10.1016/j.saa.2010.12.079.

[59] A. K. Rajasekharan, R. Bordes, C. Sandström, M. Ekh, and M. Andersson, "Hierarchical and Heterogeneous Bioinspired Composites—Merging Molecular Self-Assembly with Additive Manufacturing," *Small*, vol. 13, no. 28, pp. 1–11, 2017, doi: 10.1002/smll.201700550.

[60] F. C. Tenover and R. C. Moellering, "The Rationale for Revising the Clinical and Laboratory Standards Institute Vancomycin Minimal Inhibitory Concentration Interpretive Criteria for Staphylococcus aureus," *Clin. Infect. Dis.*, vol. 44, no. 9, pp. 1208–1215, May 2007, doi: 10.1086/513203.

[61] "Mathematical models of drug release," in *Strategies to Modify the Drug Release from Pharmaceutical Systems*, Elsevier, 2015, pp. 63–86.

[62] S. H. Lee, J. E. Lee, W. Y. Baek, and J. O. Lim, "Regional delivery of vancomycin using pluronic F-127 to inhibit methicillin resistant Staphylococcus aureus (MRSA) growth in chronic otitis media in vitro and in vivo," *J. Control. Release*, vol. 96, no. 1, pp. 1–7, Apr. 2004, doi: 10.1016/j.jconrel.2003.12.029.

[63] R. W. Korsmeyer, R. Gurny, E. Doelker, P. Buri, and N. A. Peppas, "Mechanisms of solute release from porous hydrophilic polymers," *Int. J. Pharm.*, vol. 15, no. 1, pp. 25–35, May 1983, doi: 10.1016/0378-5173(83)90064-9.

[64] A. K. Rajasekharan, C. Gyllensten, E. Blomstrand, M. Liebi, and M. Andersson, "Tough Ordered Mesoporous Elastomeric Biomaterials Formed at Ambient Conditions," *ACS Nano*, 2019, doi: 10.1021/acsnano.9b01924.